Three new species of the spider genus *Naphrys* Edwards (Araneae, Salticidae) under morphology and molecular data with notes in the distribution of *Naphrys acerba* (Peckham & Peckham) from Mexico (#104276)

First submission

Guidance from your Editor

Please submit by 29 Aug 2024 for the benefit of the authors (and your token reward) .



Structure and Criteria

Please read the 'Structure and Criteria' page for guidance.



Custom checks

Make sure you include the custom checks shown below, in your review.



Author notes

Have you read the author notes on the guidance page?



Raw data check

Review the raw data.



Image check

Check that figures and images have not been inappropriately manipulated.

If this article is published your review will be made public. You can choose whether to sign your review. If uploading a PDF please remove any identifiable information (if you want to remain anonymous).

Files

Download and review all files from the <u>materials page</u>.

- 23 Figure file(s)
- 3 Table file(s)
- 1 Raw data file(s)



DNA data checks

- Have you checked the authors data deposition statement?
- Can you access the deposited data?
- Has the data been deposited correctly?
- Is the deposition information noted in the manuscript?

Field study

! Have you checked the authors <u>field study permits</u>?

Are the field study permits appropriate?

New species checks

- Have you checked our <u>new species policies</u>?
- Do you agree that it is a new species?
- Is it correctly described e.g. meets ICZN standard?

For assistance email peer.review@peerj.com

Structure your review

The review form is divided into 5 sections. Please consider these when composing your review:

- 1. BASIC REPORTING
- 2. EXPERIMENTAL DESIGN
- 3. VALIDITY OF THE FINDINGS
- 4. General comments
- 5. Confidential notes to the editor
- You can also annotate this PDF and upload it as part of your review

When ready submit online.

Editorial Criteria

Use these criteria points to structure your review. The full detailed editorial criteria is on your guidance page.

BASIC REPORTING

- Clear, unambiguous, professional English language used throughout.
- Intro & background to show context.
 Literature well referenced & relevant.
- Structure conforms to <u>PeerJ standards</u>, discipline norm, or improved for clarity.
- Figures are relevant, high quality, well labelled & described.
- Raw data supplied (see <u>PeerJ policy</u>).

EXPERIMENTAL DESIGN

- Original primary research within Scope of the journal.
- Research question well defined, relevant & meaningful. It is stated how the research fills an identified knowledge gap.
- Rigorous investigation performed to a high technical & ethical standard.
- Methods described with sufficient detail & information to replicate.

VALIDITY OF THE FINDINGS

- Impact and novelty is not assessed.

 Meaningful replication encouraged where rationale & benefit to literature is clearly stated.
- All underlying data have been provided; they are robust, statistically sound, & controlled.



Conclusions are well stated, linked to original research question & limited to supporting results.

Standout reviewing tips



The best reviewers use these techniques

Т	p

Support criticisms with evidence from the text or from other sources

Give specific suggestions on how to improve the manuscript

Comment on language and grammar issues

Organize by importance of the issues, and number your points

Please provide constructive criticism, and avoid personal opinions

Comment on strengths (as well as weaknesses) of the manuscript

Example

Smith et al (J of Methodology, 2005, V3, pp 123) have shown that the analysis you use in Lines 241-250 is not the most appropriate for this situation. Please explain why you used this method.

Your introduction needs more detail. I suggest that you improve the description at lines 57-86 to provide more justification for your study (specifically, you should expand upon the knowledge gap being filled).

The English language should be improved to ensure that an international audience can clearly understand your text. Some examples where the language could be improved include lines 23, 77, 121, 128 – the current phrasing makes comprehension difficult. I suggest you have a colleague who is proficient in English and familiar with the subject matter review your manuscript, or contact a professional editing service.

- 1. Your most important issue
- 2. The next most important item
- 3. ...
- 4. The least important points

I thank you for providing the raw data, however your supplemental files need more descriptive metadata identifiers to be useful to future readers. Although your results are compelling, the data analysis should be improved in the following ways: AA, BB, CC

I commend the authors for their extensive data set, compiled over many years of detailed fieldwork. In addition, the manuscript is clearly written in professional, unambiguous language. If there is a weakness, it is in the statistical analysis (as I have noted above) which should be improved upon before Acceptance.



Three new species of the spider genus *Naphrys* Edwards (Araneae, Salticidae) under morphology and molecular data with notes in the distribution of *Naphrys acerba* (Peckham & Peckham) from Mexico

 $\textbf{Juan Maldonado-Carrizales}~^1, \textbf{Alejandro Valdez-Mondrag\'{o}n}~^2, \textbf{Mar\'{i}a L Jim\'{e}nez-Jim\'{e}nez}~^2, \textbf{Javier Ponce-Saavedra}~^2, \textbf{Mar\'{i}a L Jim\'{e}nez-Jim\'{e}nez}~^2, \textbf{Mar\'{i}a L Jim\'{e}nez-Jim\'{e}n$

Corresponding Author: Javier Ponce-Saavedra Email address: javier.ponce@umich.mx

Herein, we describe three new species of the spider genus *Naphrys* Edwards, 2003 from Mexico: *Naphrys echeri* **sp. nov.**, *Naphrys tecoxquin* **sp. nov.**, and *Naphrys tuuca* **sp. nov.** An integrative taxonomic approach was applied, utilizing data from morphology, ultra-morphology, molecular data (distance-based and tree-based), and distribution records. Four molecular methods for species delimitation were implemented under the corrected *p*-distance Neighbor-Joining (NJ) criteria: 1) Assemble Species by Automatic Partitioning (ASAP); 2) General Mixed Yule Coalescent (GMYC); 3) Bayesian Poisson Tree Process (bPTP); and 4) Multi-rate Poisson Tree Process (mPTP). Both morphological and molecular data supported the delimitation and recognition of the three new species. The average interspecific genetic distance (*p*-distance) within the genus *Naphrys* is 14%, while the intraspecific genetic distances (*p*-distance) is <2% for most species. We demonstrate that the natural distribution of *Naphrys* is not restricted to the Nearctic region. Furthermore, the reported localities herein represent the first with precise locations in the country for *Naphrys acerba*. In addition, a taxonomic identification key is provided for the species in the genus.

¹ Faculty of Biology, Universidad Michoacana de San Nicolás de Hidalgo, Morelia, Michoacan, Mexico

² Arachnological Collection, Centro de Investigaciones Biológicas del Noroeste, La Paz, Baja California Sur, Mexico



- 1 Three new species of the spider genus Naphrys
- 2 Edwards (Araneae, Salticidae) under morphology and
- 3 molecular data with notes in the distribution of
- 4 Naphrys acerba (Peckham & Peckham) from Mexico

Juan Maldonado-Carrizales¹, Alejandro Valdez-Mondragón², María Luisa Jiménez-Jiménez² Javier Ponce-Saavedra¹

8 9

- 10 ¹ Faculty of Biology, Entomology Laboratory, Universidad Michoacana de San Nicolás de
- 11 Hidalgo (UMSNH), Morelia, Michoacán, Mexico
- 12 ² Arachnological Collection (CARCIB), Centro de Investigaciones Biológicas del Noroeste
- 13 (CIBNOR), La Paz, Baja California Sur, Mexico

14

- 15 Corresponding Author:
- 16 Javier Ponce-Saavedra
- 17 Edificio B4 2º piso, Gral. Francisco J. Múgica S/N, Morelia, Michoacán, 58040
- 18 Email address: javier.ponce@umich.mx

19



35

36

37

38

39 40

43 44

45

46

47

48 49

50

51 52

53

54

55

56 57

58

59

Abstract

- 21 Herein, we describe three new species of the spider genus *Naphrys* Edwards, 2003 from Mexico:
- Naphrys echeri sp. nov., Naphrys tecoxquin sp. nov., and Naphrys tuuca sp. nov. An integrative 22
- taxonomic approach was applied, utilizing data from morphology, ultra-morphology, molecular 23
- data (distance based and tree based), and distribution records. Four molecular methods for 24
- species delimitation were implemented under the corrected p-distance Neighbor-Joining (NJ) 25
- 26 criteria: 1) Assemble Species by Automatic Partitioning (ASAP); 2) General Mixed Yule
- Coalescent (GMYC); 3) Bayesian Poisson Tree Process (bPTP); and 4) Multi-rate Poisson Tree 27
- 28 Process (mPTP). Both morphological and molecular data supported the delimitation and
- recognition of the three new species. The average interspecific genetic distance (p-distance) 29
- 30 within the genus Naphrys is 14%, while the intraspecific genetic distances (p-distance) is < 2%
- for most species. We demonstrate that the natural distribution of *Naphrys* is not restricted to the 31
- Nearctic region. Furthermore, the reported localities herein represent the first with precise 32
- locations in the country for Naphrys acerba. In addition, a taxonomic identification key is 33
- provided for the species in the genus. 34

Introduction

The spider family Salticidae, comprised of 6,6 described species (WSC, 2024), represents the most diverse spider family worldwide. One of the largest groups within this family is the Euophryini tribe, containing over 1,000 species within 116 genera (Edwards, 2003; Maddison, 2015; Zhang & Maddison, 2015). Euophryini species have a global distribution, 4 primarily found in tropical regions except for Africa (Zhang & Maddison, 2015; Maddison, 2015). They exhibit a remarkable uniformity in body shape, with elongate or ant-like forms uncommon. Their genitalia also share some particular characteristics: the male palp typically has a simple spiral embolus, and the epigynum has windows framed by circular folds, presumably guiding the embolus during mating (Maddison, 2015).

According to Edwards (2003), most Euophryini species in the Nearctic region are small (less than 5 mm long) with compact bodies. These species often exhibit cryptic coloration (browns or gravs) and possess a moderate number of setae on their bodies. The genus *Naphrvs* Edwards, 2003 is as a clear representative of this group. Naphrys currently includes four described species restricted to North America: Naphrys acerba (G. W. Peckham & E. G. Peckham, 1909), Naphrys bufoides (Chamberlin & Ivie, 1944), Naphrys pulex (Hentz, 1846), and Naphrys xerophila (Richman, 1981) are all found in the United States. Additionally, N. pulex extends into Canada, and N. acerba has been reported in Mexico (Richman, 1981; Edwards, 2003; WSC, 2024).

In Mexico, the distribution of N. acerba is reported in the northeastern region, but precise locations remain unclear (Richman, 1981). Nevertheless, diverse sources (Ibarra-Núñez, Mava-Morales & Chamé-Vázquez, 2011; Maddison, 2015; Maldonado-Carrizales & Ponce-Saavedra, 2017) mention the presence of the genus in different parts of Mexico without assigning known species. This highlights the limited taxonomic knowledge about this genus in the country.





The taxonomy of the tribe is encumbered by common morphological convergences and reversals, despite attempts at species delimitation using both morphological and molecular data. This taxonomic confusion is further compounded by the relative simplicity of Euophryini genitalia, which exhibit limited interspecific variation and hinder even genus-level identification (Zhang & Maddison, 2015).

Modern taxonomy enlists a wide variety of methods and different lines of evidence to analyze and delimit lineages, as morphological evidence alone can be extremely difficult or impossible to delimit species in some cases (Carstens et al., 2013, Luo et al., 2018; Nolasco & Valdez-Mondragón, 2022). This approach recognizes the limitations of relying solely on morphology.

DNA analysis has become a crucial tool in species delimitation due to its objectivity. Unlike morphology that can be subjective and influenced by the environment, DNA offers a standardized and quantifiable measure of evolutionary divergence (Fujita et al., 2012). Nevertheless, delineating or delimiting spider species based only on molecular data is insufficient and incorrect (Hamilton, Formanowicz & Bond, 2011).

The combined use of morphological and molecular data is becoming increasingly important for species delimitation in spiders. This approach is particularly valuable in families like Salticidae, where similar appearances and sexual characteristics make traditional classification methods challenging (Trębicki et al., 2021; Cala-Riquelme, Bustamante & Salgado, 2022; Maddison et al., 2022; Courtial et al., 2023; Kumar, Gupta & Sharma, 2024; Lin et al., 2024; Phung et al., 2024). Similar successes have been achieved in other spider groups such as Mygalomorphae (Hamilton et al., 2014; Ortiz & Francke, 2016; Candia-Ramírez & Francke 2021; Ferretti, Nicoletta & Soresi, 2024) and Synspermiata (Valdez-Mondragón et al., 2019; Navarro-Rodríguez & Valdez-Mondragón 2020; Navarro-Rodríguez & Valdez-Mondragón, 2024). The combined use of methods has resulted in robust characterizations of species boundaries.

The integrative taxonomy approach has emerged to address shortcomings of each method individually, using multiple data sources and disciplines in a complementary way to identify and delimit species or lineages. In other words, integrative taxonomy is the eriterion that aims to delimit species, the fundamental units of biodiversity, from different and complementary perspectives (Dayrat, 2005; DeSalle, Egan & Siddall, 2005; Padial et al., 2010; Padial & de la Riva, 2010).

While integrative taxonomy has been applied in various biological groups, its use in spider research remains limited (Bond et al., 2021). This highlights the potential for further exploration of integrative taxonomy within spider systematics.

In this study, we employ integrative taxonomy to describe three new species of the genus *Naphrys*. This approach utilizes morphological characters, ultra-morphology, and molecular data analyzed using both genetic-distance and tree-based methods for species delimitation. As there is no single species concept, in this work we employ the unified species concept, which is a flexible framework that incorporates elements from various species concepts such as the biological,



ecological, evolutionary, and phylogenetic concepts, to delimit species based on their status as separately evolving metapopulation lineages (De Queiroz, 2007; Schlick-Steiner et al., 2010). We also consider the biogeographical distribution records of the new species. Finally, we provide a taxonomic identification key for the species of the genus and accurate distribution data for *N. acerba* in northeastern Mexico.

105106

Materials & Methods

107 The specimens were collected and preserved in both 96% ethanol for molecular analyses and 80% ethanol with complete field data labels for morphological studies. Type specimens are 108 deposited at two biological collections: Colección de Arácnidos e Insectos, Centro de 109 110 Investigaciones Biológicas del Noroeste, S.C. (CARCIB), La Paz, Baja California Sur, Mexico, and Colección Aracnológica de la Facultad de Biología de la Universidad Michoacana 111 (CAFBUM), Morelia, Michoacán, Mexico. The specimens were collected under the document 112 SPARN/DGVS/074492/24, Scientific Collector Permit from the Secretaría de Medio Ambiente v 113 114 Recursos Naturales (SEMARNAT), Mexico, provided to Margarita Vargas Sandoval (Director and Head curator of the CAFBUM, Faculty of Biology, Entomology Laboratory, Universidad 115 Michoacana de San Nicolás de Hidalgo). For morphological descriptions, specimens were 116 117 observed using an Amscope SM1TZ-RL-10MA stereomicroscope. All measurements are in 118 millimeters (mm). Epigyna were dissected, manually cleaned, and temporarily cleared with clove oil following the method described by Levi (1965), after digesting the internal epigynal soft 119 tissues with KOH 10%. Left male palps were dissected and cleaned manually using hypodermic 120 needles and a small brush. Both genitalia were observed under a transmitted light microscope 121 Axiostar Plus Carl Zeiss. Habitus and genitalia photographs were obtained using separate setups, 122 123 an Amscope MU1000 camera attached to an Amscope SM1TZ-RL-10MA stereomicroscope for habitus images, and a transmitted light microscope (Axiostar Plus Carl Zeiss) for genitalia. 124 Photographs were processed with the Helicon focus v8.2.2 program and edited using Adobe 125 126 Photoshop CS6. The distribution map was created using QGIS v3.32 'Lima'. Biogeographic 127 province data (.shp) were obtained from the proposed boundaries by Morrone, Escalante & 128 Rodríguez-Tapia (2017), and Escalante, Rodríguez-Tapia & Morrone (2021). Boundary data (.shp files) were sourced from USGS (2021). Finally, the topographic base layer used was 'ESRI 129 130 Topo' via the subprogram XYZ Tiles in QGIS. For scanning electron microscopy (SEM), morphological structures were dissected, cleaned manually, dehydrated in absolute ethanol, 131 132 critical-point dried with samdri-PVT-3B equipment, and then covered with gold:palladium in a 60:40 proportion. The structures were examined under low vacuum in a Hitachi S-3000N SEM. 133 Measurements on electron micrographs are in micrometers (µm). Morphological nomenclature 134 135 mostly follows Ramirez (2014) and Zhang & Maddison (2015), with abbreviations used in the description and figures as follows: AER, anterior eyes row; PER, posterior eyes row; ALE, 136 anterior lateral eye; AME, anterior median eye; PLE, posterior lateral eye; PME, posterior 137 median eye; **OQ**, ocular quadrangle; **S**, spermatheca; **CD**, copulatory duct; **W**, window of 138 epigynum; CO, copulatory openings; FD, fertilization duct; MS, median septum; RTA, 139



retrolateral tibial apophysis; **E**, embolus; **ED**, embolic disc; **SP**, sperm pore; **T**, tegulum; **TL**, tegular lobe; **RSDL**, retrolateral sperm duct loop; **VTA**, ventral tibial apophysis; **PED**, process on embolic disc.

143 144

145

146

147

148

Taxon sampling

The molecular analyses were carried out with a total of 110 specimens, including one undescribed species of *Naphrys* and three new *Naphrys* species described herein. Because this study it is not a phylogenetic analysis, we use only one outgroup taxon to root the trees, *Corticattus latus* Zhang & Maddison, which represents the closely related genus to *Naphrys* according with Zhang & Maddison (2015) (Table 1).

149150151

152

153

154

155

156

157

158

159

160

161

162

163

164

165166

167

168

169 170

171

172

173

174

175176

177

178179

DNA extraction, amplification, and sequencing

The DNA was isolated from legs using proteinase K/phenol/chloroform following the protocol by Hillis et al. (1996). Briefly, at least 1 µL of tissue was incubated at 60°C for 24 hours with a digestion buffer containing 400 µL saline solution, 45 µL of 1% SDS solution, and 5uL of proteinase K. After digestion, 200 µL of Phenol and 200 µL of isoamyl chloroform was added and shaken vigorously. Afterwards, samples were centrifuged at 12,000 rpm for 10 minutes. Once finished, 400 uL of upper aqueous phase was recovered, repeating the phenol/chloroform washes once more. Once the phenol/chloroform washes were done, 200 uL of phenol was added to the mixture, shaken gently, and then centrifuged immediately at 12,000 rpm for 10 minutes. 300 μL of upper agueous phase was recovered and 750 μL of cold (-20°C) absolute ethanol was added. The mixture was then shaken gently and incubated for 12 hours at -20°C. Once incubated, it was centrifuged at 13,000 rpm for 20 minutes, and the ethanol was decanted by inversion, avoiding losing the bottom pellet. 600 µL of cold 70% ethanol (-20°C) was then added and centrifuged at 13,000 rpm for 20 minutes, with ethanol decanting by inversion while avoiding losing the bottom pellet. Finally, drying in a vacuum centrifuge was performed at 60°C for 10 minutes. Once the vial is dry, DNA is suspended in 50 µL of distilled water and stored at -20°C. After DNA extraction, the mitochondrial gene Cytochrome Oxidase subunit 1 (COI), proposed by Folmer et al (1994), was amplified (LCO1498 and HCO2198). Amplifications were carried out in a GeneAmp PCR System 2700 thermal cycler, in a total volume of 25.9 μL: 1.66 μL Buffer (5X), 1.5 μL MgCl2 (50 mM), 1.25 μL LCOI1498 (10 μM), 1.25 μL HCOI2198 (10 μM), 0.23 μL Tag (5U/μL), 0.875 μL dNTP's (10 mM), 1 μL BSA (1.25 mg/μL), 16.135 μL H2O, 2 μL DNA. The PCR was set up as follows: an initial step for 1 min 30 sec at 95 °C; 35 amplification cycles of 30 sec at 94 °C (denaturation), 30 sec at 50 °C (annealing), 45 sec at 72 °C (elongation), and final elongation of 10 min at 72 °C. PCR products were checked via gel electrophoresis to analyze length and purity on 1% agarose gels with a molecular marker of 100 bp.

DNA extractions were carried out at the Laboratorio de Biología Acuática "J. Javier Alvarado Díaz," while PCR amplifications were carried out at the Centro Multidiciplinario de Estudios en Biotecnología (CMEB), both at the Universidad Michoacana de San Nicolás de



Hidalgo (UMSNH) in Morelia, Michoacán, Mexico. Sequencing was carried out in Psomagen,
 Maryland, United States.

Sequence editing and alignment

The sequences were visualized in Geneious Prime v.2023.2.1 (Geneious Prime, 2023) and then manually edited using the BioEdit v. 7.7.1 program (Hall, 1999). After saving in FASTA format (.fas), the sequences were aligned using MAFFT v. 7 (Katoh & Toh 2008) with default parameters on the MAFFT online server (https://mafft.cbrc.jp/alignment/server/).

Molecular analysis and species delimitation

Four different molecular delimitation methods were employed using the corrected *p*-distances Neighbor-Joining (NJ) as initial criteria: 1) ASAP (Assemble Species by Automatic Partitioning) (Puillandre, Brouillet & Achaz, 2021), 2) GMYC (General Mixed Yule Coalescent) (Pons et al., 2006), 3) bPTP (Bayesian Poisson Tree Process) (Zhang et al., 2013), and 4) mPTP (multi-rate Poisson tree processes) (Kapli et al., 2017).

p-distances Neighbor-Joining (NJ) criteria

MEGA v.10.0.5 (Kumar et al., 2018) was used to construct the genetic distance tree, using the following parameters: number of replicates = 1000, bootstrap support values = 1000 (significant values \geq 50%), substitution type = nucleotide, model = p-distance, substitutions to include = d: transitions + transversions, rates among sites = gamma distributed with invariant sites (G+I), missing data treatment = pairwise deletion.

Assemble Species by Automatic Partitioning (ASAP)

This method is an ascending hierarchical clustering algorithm that analyzes single-locus DNA barcode datasets. It iteratively merges sequences with the highest pairwise similarity into progressively larger clusters. Additionally, ASAP retains information on all potential clustering steps, resulting in a comprehensive series of partitions representing putative species groupings within the data. Subsequently, ASAP calculates a probability score for each partition based on the within-group sequence similarity compared to between-group similarity. Finally, the method identifies the partitions with the highest probability scores as the most likely species-level groupings and constructs a species partition tree reflecting the hierarchical relationships among these putative species (Puillandre, Brouillet & Achaz, 2021). ASAP analyses were run on the online platform (https://bioinfo.mnhn.fr/abi/public/asap/) using Kimura (K80) distance matrices and configured under following parameters: substitution model = p-distances, probability = 0.01, best scores = 10, fixed seed value = -1.

General Mixed Yule Coalescent (GMYC)

The GMYC method (Fujisawa & Barraclough 2013) is a statistical framework employed for species delimitation using single-locus DNA barcode data. This approach utilizes single time



thresholds to define species boundaries within a Maximum Likelihood context, relying on ultrametric trees as input (Ortiz & Francke 2016; Nolasco & Valdez-Mondragón, 2022). Ultrametric trees were generated in this study through phylogenetic analyses performed in BEAUti and BEAST v.2.7.6 software (Bouckaert et al., 2019). A Yule Process tree prior was implemented during the analysis to account for lineage diversification patterns. Furthermore, an optimized relaxed molecular clock model was applied, incorporating the estimated evolutionary model for the COI gene (GTR + I + G). To ensure robustness of the phylogenetic inference, five independent BEAST analyses were executed, each running for 80 million iterations. Convergence of these analyses was subsequently evaluated using Tracer v1.6 (Rambaut and Drummond, 2003–2013), with a minimum threshold of 200 for the Effective Sample Sizes (ESS). Following this, Tree Annotator 2.6.0 (part of the BEAST package) was employed to generate maximum likelihood trees representing the most likely evolutionary histories. The first 25% of each independent run was discarded as burn-in to account for potential initial biases in the MCMC chains. Finally, the GMYC method was implemented through the online platform

Bayesian Poisson Tree Processes (bPTP)

(https://species.h-its.org/gmyc/) (Fujisawa & Barraclough, 2013).

bTPT operates within a Bayesian framework, accounting for uncertainties in both the phylogenetic tree's branch lengths and potential species assignments. This method assumes a Poisson process for speciation events along the tree branches and incorporates branch lengths reflecting sequence divergences. Considering this information and its inherent uncertainties, bPTP estimates posterior probabilities for various candidate species partitions within the data, which represent the likelihood of each partition accurately reflecting true species boundaries (Zhang et al., 2013). In this work, Bayesian and Maximum Likelihood variants were carried out on the online platform (https://species.h-its.org/ptp/), using following options: rooted tree, MCMC = 1000000, thinning = 100, burn-in = 0.1, seed = 123. The resulting trees were edited in FigTree 1.4.4 (Rambaut, 2018)-and Photoshop CS6. Congruence integration criteria were employed to delimit different species. This approach compares evidence across multiple methods, resulting in more robust species delimitations and better supported species hypotheses (e.g., DeSalle, Egan & Siddall, 2005; Pons et al., 2006; Navarro-Rodríguez & Valdez-Mondragón, 2020; Valdez-Mondragón, 2020; Valdez-Mondragón, 2020; Nolasco & Valdez-Mondragón, 2022).

Multi-rate Poisson Tree Processes (mPTP)

mPTP uses a non-homogeneous Poisson process model. This approach allows for the estimation of distinct rate multipliers for individual branches within the phylogenetic tree, recognizing potential heterogeneity in evolutionary rates across lineages. ML tree estimation was used to identify branch-specific rate multipliers, and Markov chain Monte Carlo (MCMC) simulations were employed to integrate over the uncertainty associated with these estimates (Kapli et al., 2017). By identifying statistically significant shifts in diversification rates along the tree generated from our ML analysis, mPTP pinpoints potential species boundaries, specifically



taking into account lineages that have undergone evolution at disparate paces. This analysis was carried out on the online platform (http://mptp.h-its.org/).

Zoobank

The electronic version of this article in Portable Document Format (PDF) will represent a published work according to the International Commission on Zoological Nomenclature (ICZN). Hence, the new names contained in the electronic version are effectively published under that Code from the electronic edition alone. This published work and the nomenclatural acts it contains have been registered in ZooBank, the online registration system for the ICZN. The ZooBank LSIDs (Life Science Identifiers) can be resolved, and the associated information viewed through any standard web browser by appending the LSIDs to the prefix http://zoobank.org/. The LSIDs for this publication are: urn:lsid:zoobank.org:act:6CFF43A9-8C98-4027-A1DA-2838FE4D79F8; urn:lsid:zoobank.org:act:D67CCC72-E17D-450C-9193-231120527FDE; and urn:lsid:zoobank.org:act:3129A3DE-57E8-46CC-8036-86DC467EB056. The online version of this work is archived and available from the following digital repositories: PeerJ, PubMed Central SCIE, and CLOCKSS:

277 Results

Molecular analysis of genetic distances

The corrected *p*-distances under NJ of COI recovered six putative species (Fig. 1). Genetic distance analyses recovered groups corresponding to one putative new species (with bootstrap support value below 50%), the two previously described species *N. pulex* and *N. xerophila* (with high bootstrap support value, 89%), and three new species described herein (with high bootstrap support value, 98%). Bootstrap support values for all species were high (>89%) (Fig. 1). The average genetic *p*-interspecific distances of *Naphrys* species was 14% (min: 11%, max: 18.1%) (Table 2). Average interspecific *p*-distance between previously known species (*N. pulex* and *N. xerophila*) was 11.8%. Between new species (*N. echeri* sp. nov., *N. tecoxquin* sp. nov., and *N. tuuca* sp. nov.) and previously known species, higher interspecific average *p*-distances were observed, between 12.9% and 14%. With average values above 15.1%, *Naphrys* sp. had the highest average interspecific *p*-distance. For most species, intraspecific distances were below 1.61%, except for *Naphrys* sp. that showed a higher value (Table 3).

Molecular methods for species delimitation

The ASAP delimitation analysis recovered all six species (*N. echeri* **sp. nov.**, *N. tecoxquin* **sp. nov.**, *N. tuuca* **sp. nov.**, *Naphrys* sp., *Naphrys* pulex, and *Naphrys xerophila*) with high (>93%) bootstrap support value (Fig. 2) from the NJ tree. GMYC and mPTP methods recovered the three new species described herein and one putative new species, while *N. pulex* was not recovered as one species (Fig. 2). The most incongruent result was observed in bPTP, which delimited 42 and 50 putative species under ML and IB variants, respectively. Only *N. tecoxquin* **sp. nov.** and *N. xerophila* were recovered by the ML variant of bPTP.



300	Only N. xerophila was recovered under all methods and supported by a high bootstrap
301	value (93%). Naphrys pulex shows the most incongruent results in all species delimitation
302	methods, recovering 10 species in mPTP, 16 in GMYC, and 42 and 50 species in the ML and BI
303	variants of bPTP method, respectively (Fig. 2). Nevertheless, N. pulex presents low intraspecific
304	genetic distance (< 2%) and high bootstrap support value (100%) (Table 3; Fig. 2).
305	
306	Taxonomy
307	Family: Salticidae Blackwall, 1841
308	Genus: Naphrys Edwards, 2003
309	
310	Type specie: Habrocestum acerbum (G. W. Peckham & E. G. Peckham, 1909)
311	
312	Emended diagnosis. After Richman (1981) and Edwards (2003). Naphrys species are
313	characterized by their small size (2–6.1 mm) and dull, cryptic coloration (black and brown)
314	(Figs. 3C-D, 6C, 12D-E, 18C-E). With one bicular d promarginal tooth on chelicera and high
315	earapace. First tibia has no more than two pairs of ventral macrosetae and leg III longer than leg
316	IV (Tibia+Patella III > Tibia+Patella IV). Male palpal bulb is usually large with a proximal TL.
317	Simple finger-like RTA and RSDL present. Also, with ventral apophysis on the palpal tibia
318	(VTA). Embolar disk (ED) has a ventral conical projection. Embolus (E) is three-dimensional
319	construction with prolateral edge of ED (Figs. 4C-H, 7C-H, 9A, 10A, 13C-H, 15A, 16A, 19C-H,
320	21A, 22A). Epigynum has a typical window structure with a median septum (Figs. 5C-F, 8C-F,
321	11, 14C-F, 17, 20C-F, 23). Copulatory openings (CO) are positioned along posterior (Figs. 20C-
322	F), median (Figs. 5C-F), or anteromedian (Figs. 8C-F, 14C-F) edges of atria, with atrial rims
323	intersecting them posteriorly. Rims fail to completely encircle the atria. Spermathecas (S) are
324	nearly spherical, more or less contiguous medially, and half or more the diameter of the atria.
325	They are positioned about halfway to entirely within the posterior part of atria as seen in ventral
326	view (Figs. 5C-F, 8C-F, 14C-F, 20C-F).
327	
328	Current composition. Naphrys is composed of seven species: Naphrys acerba (Peckham &
329	Peckham, 1909); Naphrys bufoides (Chamberlin & Ivie, 1944); Naphrys echeri sp. nov.;
330	Naphrys pulex (Hentz, 1846); Naphrys tecoxquin sp. nov.; Naphrys tuuca sp. nov.; Naphrys
331	xerophila (Richman, 1981).
332	
333	Distribution . Canada, Mexico, and the United States.
334	
335	Remarks. We emend the generic diagnosis based on copulatory organs of male and females.
336	
337	Key to Naphrys species
338	1. Male
339	Female

PeerJ

340 341	2. Dorsum of opisthosoma with two round, bright white spots (Fig. 4A)
342	3. Embolus thin and straight, larger than ED (Richman 1981; Fig. 5). White setae covering all
343	lateral side of cephalothorax (Edwards and Hill 2008; Fig. 7)
344	
345	Embolus thick and curve, shorter than ED (Richman 1981; Figs. 8, 16)
346	44
347 348 349 350 351	 4. Dorsum of the opisthosoma with a medial longitudinal white stripe that covers the anterior portion. Anterior part of cephalothorax exhibits bright, coppery bronze setae across surface (Metzner 2024; Fig. 293)
352	
353	5. Dorsum of opisthosoma with an extended medial white longitudinal band that extends across
354	the entire opisthosoma (Figs. 7A, 16C, 17A)
355	Dorsum of opisthosoma otherwise
356 357 358 359	6. Embolar disk (ED) bears a well-developed triangular process, next to the embolus, clearly visible in retrolateral view and smaller than embolus. (Figs. 7D, G, 9A-B, 10A-C). Embolus thick and shorter than ED. Cephalothorax, in dorsal view, has white setae forming a V-shape mark, extending outwards from the sides of the PLE towards the pedicel (Fig. 7A)
360 361 362 363	Embolar disk (ED) lacks a process. The thin embolus, larger than ED, folds at the midpoint, forming a gentle curve (Figs. 17E, H, 19A, 20C). Cephalothorax, in dorsal view, has white setae forming a Y-shape mark, extending outwards from the sides of the PLE (Figs. 16C, 17A)
364	
365 366 367	7. Embolus thick and curved, shorter than ED (Zhang & Maddison, 2015; Fig. 140). Anterior part of cephalothorax densely covered with a mixture of white and black setae (Edwards and Hill 2008; Fig. 8)
368	Embolus thick and straight (Fig. 12C, F, 14A, 15A). Anterior part of cephalothorax exhibits
369	bright, coppery-bronze setae
370	8. Copulatory openings (CO) are located on the external lateral side of the S (Figs. 8C, E, 13C,
371	E)
372	Copulatory openings (CO) located in different place
373	9. Pyriform S (Figs. 13C-F). Light opisthosoma with four black spots in dorsal view, along with
374	dark brown upwards chevron marks in the posterior last third (Figs. 11D, 13A)
375	
376 377	Circular S (Figs. 8C-F). Dark opisthosoma covered with coppery-bronze setae across surface and exhibiting mottled pattern of faint translucent markings (Figs. 6C, 8A)
378	



3/9	10. Copulatory ducts (CD) open into the epigynum forming transparent windows (W), with
380	openings more than one-third the length of S (Figs. 5C-F)
381	Copulatory ducts (CD) have circular opening, less than one-third the length of S. Copulatory
382	openings (CO) located anteriorly to S (Richman 1981; Fig. 18). Dark opisthosoma covered with
383	brown and black setae across surface, with a longitudinal white stripe in the middle of the first
384	third and a black chevron pattern on the remaining two-thirds (Metzner 2024; Fig. 294)
385	
386	11. Dorsum of opisthosoma with two round, bright white spots (Figs. 3C, D, 5A)
387	Dorsum of opisthosoma otherwise
388	12 Copulatory openings (CO) located in center of epigynum, touching the anterior edge of S.
389	Copulatory ducts (CD) have a unique loop, resembling a G-shape (Fig. 5C, E)
390	
391	Copulatory openings (CO) not touching anterior edge of S (Richman 1981; Fig. 22)
392	
393	13. Copulatory openings (CO) located in the middle of epigynum (Richman 1981; Fig. 10)
394	
395	Copulatory openings (CO) located in the middle basal part of epigynum (Fig. 18C, E)
396	
397	· · · · · · · · · · · · · · · · · · ·
398	Naphrys acerba (Peckham & Peckham, 1909)
399	Figs. 3–5, 21.
400	Habrocestum acerbum Peckham & Peckham, 1909, p. 522, pl. 44, figs. 1-Ic.
401	Naphrys acerba Edwards, 2003 p. 69, fig. 5-8 (Transferred from Habrocestum)
402	
403	Holotype: Holotype not assigned by author. Syntypes: several males and one female from Travis
404	County, Austin, Texas, USA, and one male from Georgia, USA. NOT EXAMINED.
405	
406	Other material examined. MEXICO: Nuevo León: 6 females (CAFBUM88003,
407	CAFBUM88004, CABUM84234, CAFBUM84242, CAFBUM84256, CAFBUM84257), along
408	path to cable car, Cerro de la Silla, Guadalupe municipality (lat. 25.655501, long100.254415,
409	587 m), oak forest, ground hand collecting, J. Maldonado Carrizales, F. Morales Martínez, E. G.
410	Fuentes Ortiz cols., 21/X/2023. <i>Tamaulipas</i> : 3 males (CAFBUM88005) and 3 immatures
411	(CAFBUM880040), Mr. Sabino's ranch, highway Ciudad Victoria-Tula km 28 (lat. 23.606512,
412	long. 99.229572, 1473 m), oak forest, ground hand collecting, J. Maldonado Carrizales, F.
413	Morales Martínez, E. G. Fuentes Ortiz cols., 20/X/2023.
414	
415	Emended diagnosis. After Peckham & Peckham (1909) and Richman (1981). Naphrys acerba
416	resembles N. bufoides and N. xerophila by possessing white, round spots on dorsal abdomen
417	(Fig. 4A-B, 5A-B). However, it differs from <i>N. xerophila</i> by lacking a medial longitudinal white
418	stripe covering anterior portion. Additionally, <i>N. acerba</i> can be distinguished from <i>N. bufoides</i>
_	1 Same Francisco Management London Company



- by its thicker embolus, which is shorter than ED (Figs. 4C-H). In females, CO of *N. acerba* are
- 420 located centrally within the epigynum, touching anterior edge of S (Figs. 5C, E). This contrasts
- with N. bufoides, where CO do not reach anterior edge of S, and N. tuuca, where CO are
- 422 positioned in middle basal part of epigynum.

- **Distribution.** UNITED STATES: Texas; MEXICO: Coahuila, Nuevo León, and Tamaulipas
- 425 (Richman, 1981).

426

- Natural history. According to Richman (1981), this species appears to be associated with oak
- 428 and juniper woodlands. Specimens used in this study were collected from upper leaf litter layer
- of oak forests (*Quercus* sp.) at 1473 m in Tamaulipas, Mexico, within known range of the
- 430 species. This also included disturbed areas into Monterrey City (Fig. 3A-D).

431

- 432 Naphrys echeri sp. nov.
- 433 Figs. 6–10, 21.
- 434 LSID: urn:lsid:zoobank.org:act:FFCFC48A-1827-4DCF-9096-DE8504E63251

435

- 436 Holotype. MEXICO. Michoacán: male from Cerro El Gigante, Jesús del Monte, Morelia
- 437 municipality (lat. 19.636605, long. -101.146877, 2192 m), oak forest (Quercus sp.), ground hand
- 438 collecting, J. Maldonado Carrizales, F. Morales Martínez, R. Cortés Santillán cols., 31/III/2023.
- 439 (CARCIB-AR-047). Allotype: Female with same data as holotype (CARCIB-Ar-008).

440

- 441 Paratypes: MEXICO: Michoacán: 1 male (CARCIB-Ar-0327) and 1 female (CARCIB-Ar-
- 442 0328), same collection data as for holotype. *Jalisco*: 1 male, 1 immature (CAFBUM84264)
- 443 Piedras Bolas, Ahualulco de Mercado municipality (lat. 20.653021, long. -104.057697, 1907 m),
- oak forest (*Quercus* sp.), ground hand collecting, J. Maldonado Carrizales, G. L. López Solís, S.
- 445 Montañez Hernández, N. Ruíz Hernández cols., 8/IV/2022, 1 female (CAFBUM88012) UMA
- Potrero de Mulas, San Sebastián del Oeste municipality (lat. 20.749852, long. -104.976763, 797
- 447 m) cloud forest, ground hand collecting, J. Maldonado Carrizales, E. G. Fuentes Ortiz cols.,
- 448 13/XII/2022.

449

- 450 Other material examined. MEXICO: Jalisco: 1 female (CNAN-Ar011468) and 1 male (CNAN-
- 451 Ar011467), beginning of the path to Cerro La Bufa, San Sebastián del Oeste municipality (lat.
- 452 20.758, long. -104.8438, 1460 m), young pine forest, D. Guerrero, G. Contreras, C. Hutton, G.B.
- 453 Edwards cols., 14/VI/2018. 3 males, 3 immatures (CNAN-Ar011464), and 1 female (CNAN-
- 454 Ar011462), Piedras Bolas, Ahualulco de Mercado municipality (lat. 20.64945, long. -104.05592,
- 455 1863 m), oak forest (*Quercus* sp.), D. Guerrero, G. Contreras, C. Hutton and G.B. Edwards cols.,
- 456 17/VI/2018.

457



Etymology. The species name "echeri" (/etʃ eri/ native pronunciation) is a noun in apposition that means "land or soil" in the P'urépecha language, referring to the microhabitat where it inhabits. The P'urépecha state, which peaked in the 14th and 15th centuries before Spanish arrival, is known today as Michoacán, and represents the type locality of this species.

462 463

464

465

466 467

468

469

470 471

472

473

474

Diagnosis. Naphrys echeri **sp. nov.** resembles N. tuuca **sp. nov.** by males having an extended medial white longitudinal line on dorsal part of opisthosoma, which extends across the entire opisthosoma (Fig. 7A). However, N. echeri **sp. nov.** differs in possessing an ED that bears a well-developed triangular process (PED) next to embolus, clearly visible in retrolateral view (Figs. 7D, G, 9B, 10A-C). Naphrys echeri **sp. nov.** has a thick and straight E shorter than ED (Figs. 7C, F), whereas in N. pulex this is thick but curved, and in N. tuuca **sp. nov.** the E is thin and folds at midpoint forming a gentle curve, ultimately larger than ED. Naphrys echeri **sp. nov.** differs from N. tecoxquin **sp. nov.** and N. tuuca **sp. nov.** in morphology of its embolus apex, with N. echeri **sp. nov.** possessing a fine projection that abruptly narrows to a spine-like structure and is oriented towards the interior of the palp (Fig. 9A-B, 10A, D). Females of N. echeri **sp. nov.** share with N. tecoxquin **sp. nov.** the placement of CO on external lateral side of S, but differ in shape; in N. echeri **sp. nov.**, S are circular (Figs. 8C-F), while in N. tecoxquin **sp. nov.** they are pyriform (Figs. 13C-F).

475 476 477

478

479 480

481

482

483 484

485

486

487 488

489

490

491

492 493

494

495

496 497 **Description. Male holotype (CARCIB-AR-047).** Total length: 2.6. Cephalothorax 1.57 long and 1.22 wide. Darkish brown, with white setae forming a V-shaped mark, extending outwards from sides of PLE towards pedicel in cephalic region (Fig. 7A). Lower border covered with white seta forming a band. Ocular quadrangle (OO) 0.3 long. Anterior eyes row (AER) 1.46 times wider than PER, AER 1.1 wide, PER 0.75 wide. Sternum reddish brown, 0.65 long, 0.5 wide. Labium reddish brown, as long as wide, 0.3 long, 0.3 wide. Endite 0.42 long, 0.17 wide, reddish brown, whitish anteriorly and square shaped (Fig. 7B). Opisthosoma 1.03 long and 0.95 wide; exhibiting a longitudinal band with white setae in dorsal view, covering more than half its width (Fig. 7A). Palp covered by white setae in dorsal view; in ventral view possesses a straight, short, and wide E that covers up to half distal part of cymbium (Figs. 7C, F, 9A, 10A). Ventral view of E with scales (Fig. 10A, C). A PED is present, easily seen in retrolateral view, triangular with fine projection on tip that abruptly narrows forming two spine-like structure (Figs. 7D, G, 9A-B, 10A-C). Embolus apex and SP are oriented towards interior of palp (Fig. 9A, 10A-B). Embolus apex presents one fine projection that abruptly narrows to a spine-like structure, while SP presents a multi-convex edge forming smooth ridges (Fig. 10D). Embolar disk (ED) completely rough and folded in anterior portion (Fig. 9A, 10A). Tegulum (T) vellow with darkish marks and wide RSDL occupying more than half of it, easily seen in retrolateral view (Figs. 7D, G). Furthermore, RSDL is divided in two, anterior loop is extremely curved forming a backwards "C" that extends from the middle of the T to its retrolateral edge. Posterior loop is curved anteriorly and straight in its most posterior part, forming a backwards "L" that does not touch retrolateral edge (Figs. 7D, G). Retrolateral tibial apophysis (RTA) wide at base, becoming



smaller in distal part slightly anteriorly oriented (Fig. 7D, G, 9B, D). Ventral tibial apophysis (VTA) rounded with a large pit at the tip. It has faint lines running across its surface (Fig. 9A, C). Reddish brown legs with black bands. Leg formula 3412. Leg I 2.84 (0.9, 0.45, 0.6, 0.46, 0.42), Leg II 2.72 (0.92, 0.45, 0.52, 0.45, 0.38), Leg III 3.9 (1.2, 0.55, 0.82, 0.77, 0.47), Leg IV 3.8 (1.3, 0.5, 0.72, 0.82, 0.45).

503 504

505

506

507

508

509

510 511

512

513

514515

516

517

Female allotype (CARCIB-Ar-008). Sexual dimorphism in coloration observed compared to male. Total length: 5.1. Cephalothorax 2.5 long and 1.9 wide. Darkish brown, with white and orange setae anteriorly (Fig. 8A). Lower border covered with white setae forming a band. Ocular quadrangle (OQ) 0.6 long. Anterior eyes row (AER) 1.27 times wider than PER, AER 1.4 wide, PER 1.1 wide. Sternum reddish brown with dark marks, 1.67 long, 0.87 wide. Labium black slightly longer than wide, 0.37 long, 0.32 wide. Endite 0.25 long, 0.65 wide, reddish brown, whitish anteriorly and ovoid shaped (Fig. 8B). Opisthosoma 2.6 long and 2.5 wide; covered with coppery bronze setae across surface and exhibiting mottled pattern of faint translucent markings (Fig. 8A). Epigynum slightly wider than long, 0.4 long, 0.34 wide. Copulatory openings (CO) located on external lateral sides of S. Circular S and a unique loop in CD forms a D-shape in each side of epigynum (Fig. 8C-F). Median septum (MS) and sides have a smooth, trident-shaped with grooves or ridges on anterior part (Fig. 10E). Windows of epigynum (W) mostly smooth, but striated centrally (Fig. 10E). Reddish brown legs with black marks. Leg formula 3412. Leg I 3.72 (1.12, 0.7, 0.85, 0.65, 0.4), Leg II 3.67 (1.3, 0.62, 0.67, 0.62, 0.45), Leg III 5.52

518519520

Distribution. MEXICO: Michoacán and Jalisco.

521

Natural history. The specimens collected inhabit oak forest (*Quercus* sp.) and cloud forest on
 litter. Adults were mainly found from March to November (Fig. 6).

524

- 525 Naphrys tecoxquin sp. nov.
- 526 Figs. 11–15, 21.
- 527 urn:lsid:zoobank.org:act:D67CCC72-E17D-450C-9193-231120527FDE

(1.85, 0.8, 1.25, 1.0, 0.62), Leg IV 4.4 (1.57, 0.67, 1.12, 0.52, 0.5).

528

- **Holotype**. MEXICO. *Jalisco*: male from Boca de Tomatlán, Cabo Corrientes municipality (lat.
- 530 20.511861, long. -105.318, 36m), tropical forest, ground hand collecting, J. Maldonado
- 531 Carrizales, R. Cortés Santillán, E. G. Fuentes Ortiz cols., 13/IV/2023 (CARCIB-Ar-048).
- Allotype Female with same data as holotype (CARCIB-Ar-009).

533

Paratypes: 1 male (CARCIB-Ar-0329) and 1 female (CARCIB-Ar-0330), same collection data as holotype; 2 males (CAFBUM84260-CAFBUM84261), 1 female (CAFBUM84238): same data as holotype.

537



Other material examined. MEXICO. *Jalisco*: 1 male (CAFBUM84232) and 12 immatures (CAFBUM84221), same collection data as holotype. 1 imm (CNAN-Ar011469), same collection data as paratype. 1 female (CNAN-Ar011471), Las Ánimas in same municipality as holotype (lat. 20.50002, long. -105.33869, 399m), tropical forest, ground hand collecting, G. Contreras col., 6/IX/2018.

Etymology. The species name "tecoxquin" (/tek'oʃkin/ native pronunciation) is a noun in apposition in reference to the original native group that inhabited an extensive region covering the entire southern coast of Nayarit and neighboring coastal of Jalisco where type locality is found.

Diagnosis. Naphrys tecoxquin **sp. nov.** males possess bright, coppery bronze setae in anterior part of cephalothorax (Figs. 11E, 12A), a light opisthosoma with four black spots in dorsal view, and dark brown upwards chevron marks in posterior last third (Fig. 12A). In contrast, *N. echeri* **sp. nov.** exhibits a dark opisthosoma covered with coppery bronze setae across its surface and displays a mottled pattern of faint translucent markings (Fig. 7A). Naphrys tecoxquin **sp. nov.** is similar to *N. xerophila*, but differs in having a thick and straight embolus (Fig. 12C-H), in contrast to the curved embolus observed in *N. xerophila* and *N. pulex. Naphrys tecoxquin* **sp. nov.** differs from *N. echeri* **sp. nov.** and *N. tuuca* **sp. nov.** in morphology of its embolus apex, which is ventrally flat and dorsally convex, oriented towards the exterior of the pedipalp. The surface of the embolus apex in *N. tecoxquin* **sp. nov.** is sinuous with small projections (Fig. 15B). Additionally, *N. tecoxquin* **sp. nov.** lacks PED next to embolus, a characteristic of *N. echeri* **sp. nov.** (Figs. 7D, G, 9B, 10A-B). In females of *N. tecoxquin* **sp. nov.**, CO are located on external lateral side of S (Fig. 13C, E). Naphrys tecoxquin **sp. nov.** differs to *N. echeri* **sp. nov.** in S shape, which is pyriform in *N. tecoxquin* **sp. nov.** (Fig. 13C-F), but round in *N. echeri* **sp. nov.** (Fig. 8C-F).

Description. Male holotype (CARCIB-Ar-048). Total length: 2.9. Cephalothorax 1.74 long and 1.26 wide. Darkish brown, with white setae forming a U-shaped mark, extending outwards from sides of PLE towards pedicel, anterior part is covered by bronze setae (Fig. 12A). Lower border covered with white setae forming a band. Ocular quadrangle (OQ), 0.6 long. Anterior eye row (AER) 1.31 times wider than PER, AER 1.18 wide, PER 0.9 wide. Sternum dark with faint yellow marks, 0.62 long, 0.46 wide. Labium dark, wider than long, 0.15 long, 0.22 wide. Endite 0.27 long, 0.25 wide, reddish brown, whitish anteriorly, and square shaped (Fig. 12B). Opisthosoma 1.16 long and 0.92 wide, exhibiting two straight longitudinal bands forming a "V" that cover almost half of anterior opisthosoma. In central part, there is a black mark in shape of three triangles joined at base. Additionally, a white diamond-shaped mark is present in distal part (Fig. 12A). Palp covered by white setae in dorsal view; in ventral view, a thick and straight E covers up to half of distal part of the cymbium (Figs. 12C, F). Embolus apex and SP are oriented towards exterior of the palp (Fig. 14A, 15A). Embolus apex is ventrally flat and dorsally convex,



oriented towards the exterior of pedipalp. Surface of the embolus apex is sinuous with small 578 projections (Fig. 15A-B). Embolar disk (ED) possesses a slight fold anteriorly, with striations at 579 center (Fig. 14A, 15A). Tegulum (T) dark with faint vellow and orange marks. RSDL wide and 580 easily seen in retrolateral view (Figs. 12D, G). Furthermore, RSDL is divided in two, anterior 581 582 loop is gently curved similar to a closed parentheses ")", extended on retrolateral edge. Adjacent, the posterior loop shares the same shape, but does not touch retrolateral edge (Figs. 12D, G). 583 Retrolateral tibial apophysis (RTA) exhibits a densely striated surface along entire length. This 584 apophysis projects in a straight orientation, gradually attenuating distally. Notably, RTA displays 585 a slight dorsal orientation relative to the palp (Fig. 14B, D). Ventral tibial apophysis (VTA) is 586 rounded and smooth (Fig. 14A, C). Femur, Patella, and Tibia of legs I and II dark with faint 587 reddish-brown marks, metatarsus amber, and tarsus vellow. Legs III and IV vellow. Leg formula 588 3412. Leg I 2.81 (0.82, 0.48, 0.62, 0.45, 0.42); leg II 2.86 (0.85, 0.47, 0.6, 0.52, 0.41); leg III 589 3.83 (1.25, 0.47, 0.77, 0.81, 0.52); leg IV 3.75 (1.27, 0.58, 0.78, 0.57, 0.52). 590

591 592

593

594

595

596

597

598

599 600

601

602

603 604

605

606

607

Female allotype (CARCIB-Ar-009). Sexual dimorphism in coloration observed compared to male. Total length: 2.68. Cephalothorax 1.5 long and 1.1 wide, darkish brown, with anterior part covered with black and orange setae (Fig. 13A); lower border covered with white setae forming a band. Ocular quadrangle (OO), 0.7 long. Anterior eyes row (AER) 1.5 times wider than PER, AER 1.08 wide. PER 0.72 wide. Sternum reddish brown with dark marks, 0.62 long, 0.46 wide. Labium black, wider than long, 0.22 long, 0.46 wide. Endite 0.28 long, 0.24 wide, reddish brown, and ovoid shaped (Fig. 13B). Opisthosoma 1.18 long and 0.92 wide; light with four black spots in dorsal view, along with dark brown upwards chevron marks in posterior last third (Fig. 13A). Epigynum longer than wide, 0.82 long, 0.46 wide. Copulatory openings (CO) are located on external lateral sides of S. Pyriform S and a unique loop in CD forms a D-shape on each side of the epigynum (Fig. 13C-F). Median septum (MS) and sides smooth, trident-shaped, with grooves on anterior edges of W (Fig. 15C). Windows of epigynum (W) longer than wide, mostly smooth, but striated at center (Fig. 15C). Reddish brown legs with black marks. Femur, Patella, and Tibia of legs I and II dark with faint reddish-brown marks, metatarsus amber, and tarsus vellow. Legs III and IV vellow with dark bands near the junction between segments. Leg formula 3412. Leg I 2.25 (0.67, 0.45, 0.47, 0.37, 0.27); leg II 2.12 (0.55, 0.4, 0.5, 0.35, 0.32); leg III 3.27 (1.05, 0.45, 0.7, 0.6, 0.47); leg IV 3.1 (1.0, 0.4, 0.67, 0.65, 0.37).

608 609 610

Distribution. MEXICO: Jalisco.

611

Natural history. The specimens collected inhabit ground above leaf litter in tropical dry forests with broad-leaved trees. Adults were mainly found from April to July and from September to November (Fig. 11).

615

616 Naphrys tuuca sp. nov.

617 Figs. 16–21.



LSID: urn:lsid:zoobank.org:act:3129A3DE-57E8-46CC-8036-86DC467EB056 618 619 620 Holotype. MEXICO. Navarit: male from Cerro San Juan, Tepic municipality (lat. 21.505877, long. -104.924464, 1121m), oak forest (*Quercus* sp.), ground hand collecting, J. Maldonado 621 622 Carrizales, R. Cortés Santillán col., 24/V/2023 (CARCIB-Ar-049). Female allotype with same data as holotype (CARCIB-Ar-010). 623 624 625 Paratypes: 2 males (CARCIB-Ar-0331; CAFBUM880039) and 2 females (CARCIB-Ar-0332; CAFBUM880021), same collection data as holotype. 626 627 628 Other material examined. MEXICO, *Navarit*: 2 males (CAFBUM880001; CAFBUM880002), 1 female (CAFBUM880075), same data as holotype. 1 male (CNAN-Ar011460), same data as 629 holotype (CNAN-Ar011461). 3 males and 3 females (CNAN-Ar011461), Ceboruco Volcano, 630 631 Jala municipality (lat. 21.1149, long. -104.5014, 1916m), wet glen, D. Guerrero, G. Contreras, C. 632 Hutton, and G.B. Edwards col., 16/V/2018. 633 **Etymology.** The species name "tuuca" (/t uuk a/ native pronunciation) is a noun in apposition 634 635 that means "spider" in the Wixárika language. Wixárika people are native to the Sierra Madre Occidental range in Navarit state, where the type locality is found. 636 637 **Diagnosis.** Cephalothorax in dorsal view of N. tuuca sp. nov. has a unique characteristic white 638 setae forming a Y-shaped mark, extending outwards from sides of PLE (Fig. 16A). In contrast, 639 640 N. echeri sp. nov. exhibits white setae forming a V-shaped mark in this region (Fig. 7A). Naphrys tuuca sp. nov. has a dark opisthosoma covered with coppery-bronze setae across 641 surface (Fig. 17A), similar to N. echeri sp. nov.; nevertheless, N. tuuca sp. nov. has a distinct 642 mottled pattern of white markings and a medial longitudinal smooth white stripe that covers 643 644 anterior portion of the opisthosoma (Fig. 17A). Males of N. tuuca sp. nov. possess a thin embolus (Fig. 17C-H). Embolus is larger than ED and folds at midpoint, forming a gentle curve 645 (Fig. 17E, H, 19A, 20A), in contrast to thin and straight embolus observed in N. bufoides. 646 Similar to Naphrys tecoxquin sp. nov., embolus apex of N. tuuca sp. nov. is curved and oriented 647 648 towards the exterior of palp. Surface of embolus apex in *N. tuuca* **sp. nov.** is smooth (Fig. 20B). Additionally, N. tuuca sp. nov. lacks PED, which is present in N. echeri sp. nov. Females of N. 649 650 tuuca sp. nov. present CO located in middle basal part of epigynum (Fig. 18C, E, 20C), differing from central location of CO observed in N. acerba, N. bufoides and N. pulex. 651 652 **Description. Male holotype (CARCIB-Ar-049).** Total length: 2.48. Cephalothorax 1.42 long 653 and 1.1 wide, dark with white setae forming a Y-shaped mark, extending outwards from sides of 654 PLE towards pedicel (Figs. 16C, 17A). Lower border covered with white setae forming a band. 655 Ocular quadrangle (OQ), 0.74 long. Anterior eye row (AER) 1.53 times wider than PER, AER 656

0.98 wide, PER 0.64 wide. Sternum dark with faint amber marks, 0.72 long, 0.5 wide. Labium

657



dark, wider than long, 0.17 long, 0.25 wide. Endite 0.35 long, 0.27 wide, amber, and square-658 shaped (Fig. 17B), Opisthosoma 1.06 long and 0.88 wide, exhibiting a longitudinal band with 659 white setae in dorsal view, covering one third of width (Fig. 16C, 17A). Palp covered by white 660 setae in dorsal view, with a thin embolus in ventral view, larger than ED, which folds at 661 662 midpoint, forming a gentle curve (Figs. 17C-H, 19A, 20A). Embolus apex exhibits a lateral flattening, resulting in a dorsally convex shape; oriented outwards from the main body of the 663 palp. Embolus apex surface with smooth contours (Fig. 20A-B). Embolar disk (ED) exhibits 664 unfolded anterior margin, and central region displays a higher concentration of striations (Fig. 665 20A, 21A). Tegulum (T) dark with faint yellow and orange marks, RSDL wide, easily seen in 666 retrolateral view (Figs. 17D, G). Furthermore, RSDL is divided in two, with anterior loop 667 extremely curved, forming a backwards "C" that extends from middle of T to its retrolateral 668 edge. Posterior loop is curved anteriorly and straight in its most posterior part, forming a hooked-669 shape that does not touch retrolateral edge (Figs. 17D, G). Retrolateral tibial apophysis (RTA) 670 671 exhibits sparse striations along its entire length. This structure projects in a straight orientation, gradually attenuating distally and displaying a slight anterior orientation (Fig. 17D, G, 19B, D). 672 Ventral tibial apophysis (VTA) presents a conical structure with a roughened surface texture and 673 a small notch distally (Fig. 19A, C). Yellow legs with black bands. Leg formula 3412. Leg I 2.71 674 (0.78, 0.47, 0.50, 0.49, 0.45); leg II 2.68 (0.96, 0.45, 0.51, 0.50, 0.24); leg III 3.91 (1.26, 0.65, 675 0.78, 0.74, 0.47); leg IV 3.6 (1.1, 0.45, 0.76, 0.87, 0.49). 676

677 678

679 680

681

682

683 684

685

686

687 688

689

690

691

692

693

694

Female allotype (CARCIB-r-010). Sexual dimorphism in coloration observed compared to male. Total length: 3.64. Cephalothorax 1.64 long and 1.34 wide, darkish brown, anterior part covered with white and orange setae (Fig. 16D, 18A). Lower border covered with white setae forming a band. Ocular quadrangle (OQ) 0.68 long. Anterior eyes row AER 1.47 times wider than PER, AER 1.18 wide, PER 0.8 wide. Sternum reddish brown with dark marks, 0.67 long, 0.57 wide. Labium dark with faint amber marks, wider than long, 0.2 long, 0.27 wide. Endite 0.37 long, 0.25 wide, reddish brown, and ovoid shaped (Fig. 18B). Opisthosoma 2.0 long and 1.8 wide, dark, covered with coppery-bronze setae across surface, with a mottled pattern of white markings and a medial longitudinal smooth white stripe covering anterior portion (Fig. 18A). Epigynum slightly wider than long, 0.3 long, 0.34 wide. Copulatory openings (CO) located in middle basal part of epigynum. Circular S and a unique loop in CD form a D-shape in each side of epigynum (Fig. 18C-F). Median septum (MS) exhibits a smooth surface texture, while anterior edges of W present grooves (Fig. 20C). Overall surface of W exhibits a slightly roughened texture. Windows of epigynum (W) as long as wide (Fig. 20C). Legs yellow with dark marks, metatarsus amber, and tarsus yellow. Legs III and IV yellow with dark bands near segment junctions. Leg formula 3412. Leg I 2.82 (0.88, 0.52, 0.56, 0.5, 0.36); leg II 2.86 (0.92, 0.44, 0.58, 0.58, 0.34); leg III 4.14 (1.34, 0.58, 0.82, 0.9, 0.5); leg IV 4.06 (1.3, 0.56, 0.8, 0.82, 0.58).

695 696 697

Distribution. MEXICO: Nayarit.



701

708

 Natural history. The specimens collected inhabit ground above leaf litter in oak forests (*Quercus* sp.). Adults were mainly found from May to September. This species feeds on small animals such as Collembola (Fig. 16D).

Discussion

Species delimitation within the family Salticidae has increasingly relied on a combination of molecular and morphological data. This trend is evident in studies that employ a phylogenetic perspective (Maddison, 2016a, 2016b; Cala-Riquelme, Bustamante & Salgado, 2022; Maddison et al., 2022). While genomic data can also be a reliable approach (Kanesharatnam & Benjamin, 2021; Lin, Yang & Zhang, 2024), it typically requires greater resource investments and analysis time. In contrast, studies integrating diverse data sources for species delimitation within Salticidae remain relatively scarce.

A notable example is the work by Trębicki et al. (2021), who addressed taxonomic ambiguities within the genus *Cytaea* and related species. The authors attributed this taxonomic confusion to poor original diagnoses and descriptions within the genus. To resolve this issue, Trębicki et al. (2021) employed a combined approach, analyzing both the morphology of the holotype specimens and utilizing the Automatic Barcode Gap Detection (ABGD) method based on a NJ tree constructed with COI gene sequences. Their results revealed that previously recognized "similar species" were synonymous with the *Cytaea* holotype, prompting the authors to formally synonymize these taxa.

While the authors employed a distance-based delimitation method (NJ tree) to clarify the identity of ambiguous species, in our work we take a more comprehensive approach, incorporating tree-based molecular analyses. To avoid future confusion, we also present an emended diagnosis of the genus *Naphrys*. These comprehensive resources aim to facilitate accurate species and genus-level determinations.

Boperachchi et al. (2022) further exemplify the application of molecular methods for species delimitation within Salticidae. Their study aimed to clarify the species diversity within the genus *Ballus* in Sri Lanka. Three species had been previously reported for this region, described in the late 19th and early 20th centuries. To address this taxonomic uncertainty, Boperachchi et al. (2022) employed a multifaceted approach, integrating morphological data with sequence data from three genes (COI, H3, 28S). They utilized multiple species delimitation methods, including ABGD, mPTP, and Bayesian Multi-Locus Species Delimitation (BPP). Notably, all applied methods yielded congruent results, indicating that the three previously recognized *Ballus* species represented a single species with consistent morphological characteristics and no significant genetic differentiation.

Similar to our work, the authors employed multiple molecular methods to investigate species diversity within a genus containing previously described species. In our study, the mPTP method, also used by Boperachchi et al. (2022), not only confirmed the identity of the previously known species *N. xeophila*, but also supported the designation of three new species.



Finally, Phung et al. (2024) employed a combined approach for species delimitation within the genus *Phintella* and related *Phintella*-like spiders. Their approach utilized three distinct methods: one distance-based method (ASAP) and two tree-based methods (Bayesian version of GMYC and BPP). These methods were used to delineate putative new species based on available genetic data. Furthermore, the authors recognized the challenge of strong sexual dimorphism within *Phintella*. They addressed this limitation by incorporating the same methods to assign male-female combinations for approximately one-third of the species where such pairings were unknown. The analyses by Phung et al. (2024) resulted in the identification of 22 distinct species, with 11 potentially representing undescribed taxa. Nevertheless, it is important to note that the study did not formally establish new species through the nomenclatural act.

Concordant with our findings, Phung et al. (2024) applied various methods for species delimitation. The distance-based ASAP method yielded a lower species count similar to our results. Conversely, tree-based methods (bGMYC and BPP) led to overestimations, as we also observed. Both studies endorse the utility of the COI gene for preliminary detection of potentially undescribed species, which subsequently have to be described as performed in this work.

Similar to the challenges encountered in the previous discussed studies, the Euophryini tribe exhibits numerous taxonomic uncertainties. These difficulties often stem from poor original species descriptions, limited knowledge of sexual dimorphism (e.g., only one sex known for some species), and high morphological similarity among species. To overcome these limitations, researchers have increasingly employed a combination of multiple methods (e.g., morphological and molecular data) for species delimitation (Navarro-Rodríguez & Valdez-Mondragón, 2020; Candia-Ramírez & Francke 2021; Cala-Riquelme, Bustamante & Salgado, 2022).

Morphological characters, particularly sexual characteristics, remain indispensable for robust species diagnosis, identification, and delimitation (Valdez-Mondragón, 2020). This is due, in part, to the typically low level of intraspecific variation and high level of interspecific variation observed in spider genitalia (Eberhard, 1985; Eberhard et al., 1998), making this characteristic a valuable diagnostic tool (Valdez-Mondragón, 2013; 2020; Valdez-Mondragón & Francke, 2015). In our study, we delimited different species through morphological characters, some of which were particularly diagnostic. For instance, the presence of a clearly visible PED in *N. echeri* sp. nov. and the distinctive shape of S readily distinguished this species from its congeners.

Modern taxonomic practices increasingly emphasize the integration of multiple data sources for species validation and delimitation. This combined approach strengthens the evidence for species boundaries and provides a more comprehensive understanding of the newly described taxa. In this way, the study herein represents the first where new species are described within the Salticidae family through species delimitation methods based on molecular data (both distance and tree-based).

Compared to other genes, the use of the COI gene has proven to be an effective tool for species delimitation in spiders (Trebicki et al., 2021; Valdez-Mondragón et al., 2019; Navarro-



Rodríguez & Valdez-Mondragón, 2020; Nolasco & Valdez-Mondragón, 2022; Phung et al.. 2024). Naseem & Muhamman (2016) identified Salticidae in citrus orchards using the COI gene with interspecific values of nucleotide divergence between 9.96–11.91%. Yamasaki et al. (2018) found higher interspecific values of nucleotide divergence (14.1–18.2%) in their redescription of the genus Chrysilla, based on morphology and DNA barcoding. Those studies serve as a reference for variation among different species. The interspecific genetic divergences found in this work were greater than 11% (mean: 14%, min: 11%, max: 18.1%), fitting within the range previously reported for Salticidae.

For many taxonomic groups, a 3% genetic divergence threshold is often used to define species boundaries (Sbordoni, 2010). However, this value can vary across animal groups and even among closely related species due to differences in evolutionary rates (Trębicki et al., 2021). Previous studies (Vink, Dupérré & McQuillan, 2011; Richardson & Gunter, 2012; Blagoev et al., 2016; Trębicki et al., 2021) have reported a broad range of intraspecific genetic divergences within the Salticidae family, ranging from less than 0.5% to 7.57%.

Our results (Table 3) fit within this established range for Salticidae, except for *Naphrys* sp., which exhibited a higher divergence value of 10.94%. Nevertheless, the use of genetic data obtained from GenBank for this taxon precluded a morphological examination to identify diagnostic characters. Of note is *Naphrys pulex*, which despite inconsistencies in some species delimitation methods, showed observed intraspecific variation less than 2%, which falls well within the expected range for species of Salticidae.

Among the methods tested in this work, ASAP recovered the lowest number of species, similar to the findings by Phung et al. (2024) with Salticidae. Guo & Kong (2022) suggested that the distance-based approach is generally superior to the tree-based approach, with the ASAP method being the most efficient. As in Phung et al. (2024), our use of GMYC, bPTP, and mPTP methods resulted in a significantly higher number of delineated species. This contrast to previous studies with other groups (Mygalomorphae and Araneomorphae) of spiders (Ortiz & Francke, 2016; Valdez-Mondragón et al., 2019; Navarro-Rodríguez & Valdez-Mondragón, 2020), in which a lower number of species were typically identified using similar methods. This discrepancy might be attributed to the limitations of GMYC and PTP methods. As discussed by Luo et al. (2018) and Guo & Kong (2022), these methods can be particularly sensitive to gene flow, which can disrupt the clear correlation between population size and divergence time, potentially leading to an overestimation of species boundaries. This overestimation issue could explain the differences found in the tree-based methods of the molecular analysis for *N. pulex*, despite the low genetic intraspecific distances observed (<2%).

Hamilton, Formanowicz & Bond (2011) emphasized the utility of geographical data in species delimitation. In our study, the different *Naphrys* species present in Mexico can be separated by their distribution. *Naphrys pulex* is widespread throughout the biogeographic Alleghany subregion corresponding to eastern Canada and the United States (Escalante, Rodríguez-Tapia & Morrone, 2021). *Naphrys xerophila* is distributed only in the southeastern coastal plains of the United States through the Austroriparian biogeographic province within the



Alleghany subregion (Richman, Cutler & Hill, 2012; Escalante, Rodríguez-Tapia & Morrone, 2021). Their distribution is limited by the increased aridity in the western and southern boundaries of the Alleghany subregion (Takhtajan, 1986; Escalante, Rodríguez-Tapia & Morrone, 2021).

Prior to this study, the only known species present in Mexico was *N. acerba*, which is distributed in the northern part of the Sierra Madre Oriental biogeographical province in the northeast of the country. *Naphrys tecoxquin* **sp. nov.** inhabits a distinct biogeographical province, the Pacific Lowlands. This province corresponds to a narrow, uninterrupted strip along the Pacific coast (Morrone, 2019). *Naphrys tuuca* **sp. nov.** and *N. echeri* **sp. nov.** are distributed within the Trans-Mexican Volcanic Belt (TVB) province. This province corresponds to the set of volcano mountain ranges that traverses the country from west to east (Morrone, 2019).

Within the TVB, *N. tuuca* **sp. nov.** inhabits the western mountain zone. In contrast, *N. echeri* **sp. nov.** occupies the central mountains of the TVB. *Naphrys echeri* **sp. nov.** also occurs in the eastern mountains of Mexico, specifically in the northern part of the Sierra Madre del Sur (SMS) province, a mountain system that runs in parallel to the Pacific Ocean coast in a northwest-southeast direction. Nevertheless, its continuity is interrupted by a series of valleys, with rivers typically flowing above 1000 m (Hernández-Cerda, Azpra-Romero & Aguilar-Zamora, 2016; Morrone, 2019). The SMS and TVB provinces are both part of the Mexican Transition Zone (MTZ). The MTZ exhibits a unique combination of characteristics that distinguish it from other transition zones. Notably, it harbors a remarkable mixture of Nearctic and Neotropical taxa.

Geographical barriers play a key role in the differential distribution of *N. echeri* **sp. nov.** and *N. tuuca* **sp. nov.** The SMS mountain range breaks through a tectonic graben of volcanic plateaus, with stratovolcanoes developing along its margins such as the Ceboruco Volcano (Blanco y Correa, Pérez & Cruz-Medina, 2021). The easternmost locality for *N. tuuca* **sp. nov.** is separated from western localities of *N. echeri* **sp. nov.** (Piedras Bolas in the TVB and Potrero de Mulas in the SMS) by extensive alluvial plains (up to 25 km wide) and deep clefts formed by the Ameca River (Valdivia-Ornelas & Castillo-Aja, 2001; Blanco y Correa, Pérez & Cruz-Medina, 2021; Valero-Padilla, Rodríguez-Revnaga & Cruz-Angón, 2017).

The species described herein are the southernmost representatives of the genus. Contrary to prior assumptions by Edwards (2003) that the genus has a Nearctic distribution, our findings reveal the presence of these species in the Neotropical region, suggesting a broader geographical range. While the present work focused on western Mexico, further exploration particularly in the south is likely to yield additional undescribed species. This study also provides the first precise locality data for *N. acerba* within Mexico, previously known only from historical records.

Our study demonstrates the utility of the COI gene for robust species-level delimitation within the *Naphrys* genus. This finding is supported by the high congruence observed among most methods employed. Additionally, morphological characters, particularly the male palps and female epigynes, proved to be reliable features for the identification and diagnosis of *Naphrys* species.

PeerJ

857	
858	Acknowledgements
859	The first author thanks the Consejo Nacional de Humanidades, Ciencia y Tecnología
860	(CONHACYT) of Mexico for the scholarship (no. 790303) to carry out their PhD studies. The
861	first author also thanks the Programa Institucional de Doctorado en Ciencias Biológicas
862 863	(PIDCB), Facultad de Biología, Universidad Michoacana de San Nicolás de Hidalgo (UMSNH), for the academic training during the research, as well as to the PhD synodal committee for their
864	valuable contributions, comments, and suggestions in the realization of this work. The authors
865	appreciate the support of technician Ariel Arturo Cruz Villacorta in the operation of the Scanning
866	Electron Microscope (SEM) in the Electron Microscopy Laboratory at Centro de Investigaciones
867	Biológicas del Noroeste, S.C.
868	Defevered
869 870	References Bidegaray-Batista L, Arnedo MA. 2011. Gone with the plate: the opening of the Western
871	Mediterranean basin drove the diversification of ground-dweller spiders. BMC
872	Evolutionary Biology, 11(317): 1-15. https://doi.org/10.1186/1471-2148-11-317
873	Blagoev GA, deWaard JR, Ratnasingham S, deWaard L, Lu L, Robertson J, Telfer AC, Hebert
874	DN. 2016. Untangling taxonomy: A DNA barcode reference library for Canadian spiders.
875	Molecular Ecology Resources, 16: 325–341. https://doi.org/10.1111/1755-0998.12444
876	Blanco y Correa M, Pérez MAO, Cruz-Medina J. 2021. Diversidad del relieve. In: Angón AC,
877	Medina JC, Cordero, KCN, Melgarejo ED, Fong JAS, Uribe EYF, ed. La biodiversidad en
878	Nayarit. Estudio de Estado. Vol. I. México: CONABIO, 40-45.
879	Bond JE, Godwin RL, Colby JD, Newton LG, Zahnle XJ, Agnarsson I, Hamilton CA, Kuntner M.
880	2021. Improving taxonomic practices and enhancing its extensibility—an example from
881	araneology. Diversity, 14(1): 1-15. https://doi.org/10.3390/d14010005
882	Bouckaert R, Vaughan TG, Barido-Sottani J, Duchêne S, Fourment M, Gavryushkina A, Heled J,
883	Jones G, Kühnert D, De Maio N, Matschiner M, Mendes FK, Müller NF, Ogilvie HA,
884	duPlessis L, Popinga A, Rambaut A, Rasmussen D, Siveroni I, Suchard MA, Wu CH, Xie
885	D, Zhang C, Stadler T, Drummond AJ. 2019. BEAST2.5: An advanced software platform
886	for Bayesian evolutionary analysis. PLoS Computational Biology, 15(4): e1006650.
887	https://doi.org/10.1371/journal.pcbi.1006650
888	Cala-Riquelme F, Bustamante AA, Salgado A. 2022. Morphological delimitation of the genus
889	Cobanus F.O. Pickard-Cambridge, 1900 (Araneae: Salticidae: Euophryini) with a



390	description of two new species from Colombia. Zoologischer Anzeiger, 297: 42-70.
391	https://doi.org/10.1016/j.jcz.2022.02.002
392	Candia-Ramírez D, Francke O. 2021. Another stripe on the tiger makes no difference? Unexpected
393	diversity in the widespread tiger tarantula Davus pentaloris (Araneae: Theraphosidae:
394	Theraphosinae). Zoological Journal of the Linnean Society, 192(1): 75-104.
395	https://doi.org/10.1093/zoolinnean/zlaa107
396	Carstens BC, Pelletier TA, Reid NM, Satler J. 2013. How to fail at species delimitation. Molecular
397	Ecology, 22(17): 4369-4383. https://doi.org/10.1111/mec.12413
398	Courtial C, Privet K, Aubriot X, Picard L, Pétillon J. 2023. Description of a new species of
399	Hypaeus (Araneae: Salticidae: Salticinae: Amycini) based on integrative taxonomy.
900	Studies on Neotropical Fauna and Environment, 58(2): 439-447.
901	https://doi.org/10.1080/01650521.2022.2068223
902	Dayrat B. 2005. Towards integrative taxonomy. Biological journal of the Linnean society, 85(3):
903	407-417. https://doi.org/10.1111/j.1095-8312.2005.00503.x
904	De Queiroz K. 2007. Species concepts and species delimitation. Systematic biology, 56(6): 879-
905	886. https://doi.org/10.1080/10635150701701083
906	DeSalle R, Egan MG, Siddall M. 2005. The unholy trinity: taxonomy, species delimitation and
907	DNA barcoding. Philosophical Transactions of the Royal Society B: Biological Sciences,
809	360:1905-1916. https://doi.org/10.1098%2Frstb.2005.1722
909	Dimitrov D, Arnedo MA, Ribera C. 2008. Colonization and diversification of the spider genus
910	Pholcus Walckenaer, 1805 (Araneae, Pholcidae) in the Macaronesian archipelagos:
911	evidence for long-term occupancy yet rapid recent speciation. Molecular phylogenetics and
912	evolution, 48(2): 596-614. https://doi.org/10.1016/j.ympev.2008.04.027
913	Dimitrov D, Hormiga G. 2021. Spider diversification through space and time. Annual Review of
914	Entomology, 66: 225-241. https://doi.org/10.1146/annurev-ento-061520-083414
915	Eberhard WG. 1985. Sexual Selection and Animal Genitalia. Cambridge: Harvard university Press.
916	https://doi.org/10.4159/harvard.9780674330702
917	Eberhard WG, Huber BA, Rodriguez RL, Briceno RD, Salas I, Rodriguez V. 1998. One size fits
918	all? Relationships between the size and degree of variation in genitalia and other body parts
919	in twenty species of insects and spiders. Evolution, 52: 415-431.
920	https://doi.org/10.1111/j.1558-5646.1998.tb01642.x



- 921 Eberle J, Dimitrov D, Valdez-Mondragón A, Huber BA. 2018. Microhabitat change drives
- diversification in pholcid spiders. BMC Evolutionary Biology, 18: 1-13.
- 923 https://doi.org/10.1186/s12862-018-1244-8
- 924 Edwards GB, Hill DE. 2008. Representatives of the North American salticid fauna, revisited.
- 925 Peckhamia, 30.2: 1-15.
- 926 Edwards GB. 2003. A review of the Nearctic jumping spiders (Araneae: Salticidae) of the
- 927 subfamily Euophryinae north of Mexico. Insecta Mundi, 16(2002): 65-75.
- 928 Escalante T, Rodríguez-Tapia G, Morrone JJ. 2021. Toward a biogeographic regionalization of
- 929 the Nearctic region: Area nomenclature and digital map. Zootaxa, 5027(3): 351–375.
- 930 https://doi.org/10.11646/zootaxa.5027.3.3
- 931 Ferretti N, Nicoletta M, Soresi DS. 2024. An integrative taxonomy approach evaluates the limits
- of the widespread tarantula *Plesiopelma longisternale* (Araneae: Mygalomorphae:
- Theraphosidae) and reveals a new species from Argentina. Zoologischer Anzeiger, 308:
- 934 131-143. https://doi.org/10.1016/j.jcz.2023.12.003
- 935 Folmer M, Black W, Lutz R, Vrijenhoek R. 1994. DNA primers for amplification of mitochondrial
- 936 cytochrome c oxidase subunit I from diverse metazoan invertebrates. Molecular Marine
- Biology and Biotechnology, 3: 294–299.
- 938 Fujisawa T, Barraclough TG. 2013. Delimiting species using single-locus data and the Generalized
- 939 Mixed Yule Coalescent approach: A revised method and evaluation on simulated data sets.
- 940 Systematic Biology, 62(5): 707–724. https://doi.org/10.1093/sysbio/syt033
- 941 Fujita MK, Leaché AD, Burbrink FT, McGuire JA, Moritz C. 2012. Coalescent-based species
- delimitation in an integrative taxonomy. Trends in ecology & evolution, 27(9): 480-488.
- 943 https://doi.org/10.1016/j.tree.2012.04.012
- 944 Geneious Prime. 2023. Geneious Prime 2023.2.1. Available at https://www.geneious.com
- 945 (accesed 10 October 2023).
- 946 Guo B, Kong L. 2022. Comparing the Efficiency of Single-Locus Species Delimitation Methods
- 947 within Trochoidea (Gastropoda: Vetigastropoda). Genes, 13: 2273.
- 948 https://doi.org/10.3390/genes13122273
- 949 Hall TA. 1999. BioEdit: a user-friendly biological sequence alignment editor and analysis program
- 950 for Windows 95/98/NT. [Abstract] Nucleic acids symposium series 47: 95-98.



951	Hamilton CA, Formanowicz DR, Bond JE. 2011. Species delimitation and phylogeography of
952	Aphonopelma hentzi (Araneae, Mygalomorphae, Theraphosidae): Cryptic diversity in
953	North American tarantulas. PLoS ONE, 6(10): e26207.
954	https://doi.org/10.1371/journal.pone.0026207
955	Hamilton CA, Hendrixson BE, Brewer MS, Bond JE. 2014. An evaluation of sampling effects on
956	multiple DNA barcoding methods leads to an integrative approach for delimiting species:
957	A case study of the North American tarantula genus Aphonopelma (Araneae,
958	Mygalomorphae, Theraphosidae). Molecular Phylogenetics and Evolution, 71: 79-93.
959	https://doi.org/10.1016/j.ympev.2013.11.007
960	Hernández-Cerda ME, Azpra-Romero E, Aguilar-Zamora V. 2016. Condiciones climáticas de la
961	Sierra Madre del Sur. In: Luna-Vega I, Espinosa D, Contreras-Medina R, ed. Biodiversidad
962	de la Sierra Madre del Sur: una síntesis preliminar. México: UNAM, 91-116.
963	Ibarra-Núñez G, Maya-Morales J, Chamé-Vázquez D. 2011. Las arañas del Bosque Mesófilo de
964	Montaña de la Reserva de la Biosfera Volcán Tacaná, Chiapas, México. Revista Mexicana
965	de Biodiversidad, 82(4): 1183-1193. https://doi.org/10.22201/ib.20078706e.2011.4.736
966	Jackson ND, Carstens BC, Morales AE, O'Meara BC. 2017. Species delimitation with gene flow.
967	Systematic biology, 66(5): 799-812. https://doi.org/10.1093/sysbio/syw117
968	Kanesharatnam N, Benjamin SP. 2021. Phylogenetic relationships and systematics of the jumping
969	spider genus <i>Colopsus</i> with the description of eight new species from Sri Lanka (Araneae:
970	Salticidae). Journal of Natural History, 54(43-44): 2763-2814.
971	http://dx.doi.org/10.1080/00222933.2020.1869335
972	Kapli P, Lutteropp S, Zhang J, Kobert K, Pavlidis P, Stamatakis A, Flouri T. 2017. Multi-rate
973	Poisson tree processes for single-locus species delimitation under maximum likelihood and
974	Markov chain Monte Carlo. Bioinformatics, 33(11): 1630-1638.
975	https://doi.org/10.1093/bioinformatics/btx025
976	Katoh K, Toh H. 2008. Recent developments in the MAFFT multiple sequence alignment program.
977	MAFFT version 7. Briefings in Bioinformatics, 4(4): 286–298.
978	https://doi.org/10.1093/bib/bbn013
979	Kumar R, Gupta BK, Sharma AK. 2024. Revisiting taxonomic problems in the genus <i>Myrmaplata</i>
980	Prószyński, 2016 (Araneae: Salticidae). International Journal of Entomology Research,
981	9(1): 7-14. https://dx.doi.org/10.2139/ssrn.4334501



- 982 Kumar S, Stecher G, Li M, Knyaz C, Tamura K. 2018. MEGA X: Molecular evolutionary genetics 983 analysis across computing platforms. Molecular Biology and Evolution, 35(6): 1547-1549. 984 https://doi.org/10.1093/molbev/msy096 Levi HW. 1965. Techniques for the study of spider genitalia. Psyche: A Journal of entomology, 985 72: 152-158. https://doi.org/10.1155/1965/94978 986 987 Lin L, Yang ZY, Zhang JX. 2024. Revalidation of the jumping spider genus *Cheliceroides* Zabka, 988 1985 based on molecular and morphological data (Araneae, Salticidae). ZooKeys, 1196: 989 243-253. https://doi.org/10.3897/zookeys.1196.117921 990 Luo A, Ling C, Ho YM, Zhu CD. 2018. Comparison of methods for molecular species delimitation across a range of speciation scenarios. Systematic Biology, 67(5): 830-846. 991 https://doi.org/10.1093/sysbio/syy011 992 Maddison WP, Ruiz GRS, Ng PYC, Vishnudas EH, Sudhikumar AV. 2022. Kelawakaju gen. nov., 993 994 a new Asian lineage of marpissine jumping spiders (Araneae, Salticidae, Marpissina). 995 ZooKeys, 1130: 79-102. https://doi.org/10.3897/zookeys.1130.87730 Maddison WP. 2015. A phylogenetic classification of jumping spiders (Araneae: Salticidae). 996 997 Journal of Arachnology, 43(3): 231-292. https://doi.org/10.1636/arac-43-03-231-292 Maddison WP. 2016a. Sumakuru, a deeply-diverging new genus of lyssomanine jumping spiders 998 614: 87-96. 999 from **Ecuador** (Araneae: Salticidae). ZooKeys, 1000 http://dx.doi.org/10.3897/zookeys.614.9368 1001 Maddison WP. 2016b. Papuaneon, a new genus of jumping spiders from Papua New Guinea
- 1002 (Araneae: Salticidae: Neonini). Zootaxa, 4200(3): 437-443.

 1003 http://dx.doi.org/10.11646/zootaxa.4200.3.9
- Maldonado-Carrizales J, Ponce-Saavedra J. 2017. Arañas Saltarinas (Araneae: Salticidae) en dos sitios contrastantes en grado de antropización en Morelia Michoacán, México. Entomología mexicana, 4(1), 597-603.
- Metzner H. 2024. Jumping spiders (Arachnida: Araneae: Salticidae) of the world. Available at https://www.jumping-spiders.com (accessed 20 March 2024).
- Morrone JJ, Escalante T, Rodríguez-Tapia G. 2017. Mexican biogeographic provinces: Map and shapefiles. Zootaxa, 4277(2): 277–279. https://doi.org/10.11646/zootaxa.4277.2.8



1011	Morrone JJ. 2019. Regionalización biogeográfica y evolución biótica de México: encrucijada de
1012	la biodiversidad del Nuevo Mundo. Revista Mexicana de Biodiversidad, 90: e902980.
1013	https://doi.org/10.22201/ib.20078706e.2019.90.2980
1014	Naseem S, Muhamman HT. 2016. Use of mitochondrial COI gene for the identification of family
1015	Salticidae and Lycosidae of spiders. Mitochondrial DNA Part A, 29: 96-101.
1016	http://dx.doi.org/10.1080/24701394.2016.1248428
1017	Navarro-Rodríguez CI, Valdez-Mondragón A. 2024. Violins we see, species we don't Species
1018	delimitation of the spider genus Loxosceles Heineken & Lowe (Araneae: Sicariidae) from
1019	North America using morphological and molecular evidence. Zootaxa, 5428 (4): 527-548
1020	https://doi.org/10.11646/zootaxa.5428.4.4
1021	Navarro-Rodríguez I, Valdez-Mondragón A. 2020. Description of a new species of Loxosceles
1022	Heineken & Lowe (Araneae, Sicariidae) recluse spiders from Hidalgo, Mexico, under
1023	integrative taxonomy: Morphological and DNA barcoding data (CO1+ITS2). European
1024	Journal of Taxonomy, 704: 1-30. https://doi.org/10.5852/ejt.2020.704
1025	Nolasco S, Valdez-Mondragón A. 2022. To be or not to be Integrative taxonomy and species
1026	delimitation in the daddy long-legs spiders of the genus <i>Physocyclus</i> (Araneae, Pholcidae)
1027	using DNA barcoding and morphology. ZooKeys, 1135: 93-118.
1028	https://doi.org/10.3897/zookeys.1135.94628
1029	Ortiz D, Francke O. 2016. Two DNA barcodes and morphology for multi-method species
1030	delimitation in Bonnetina tarantulas (Araneae: Theraphosidae). Molecular Phylogenetics
1031	and Evolution, 101: 176–193. https://doi.org/10.1016/j.ympev.2016.05.003
1032	Padial JM, De La Riva I. 2010. A response to recent proposals for integrative taxonomy. Biological
1033	Journal of the Linnean Society, 101(3): 747-756. https://doi.org/10.1111/j.1095-
1034	8312.2010.01528.x
1035	Padial JM, Miralles A, De la Riva I, Vences M. 2010. The integrative future of taxonomy. Frontiers
1036	in zoology, 7: 1-14. https://doi.org/10.1186/1742-9994-7-16
1037	Phung LTH, Su YC, Yamasaki T, Li YY, Eguchi K. 2024. High species diversity of <i>Phintella</i> and
1038	Phintella-like spiders (Araneae: Salticidae) in Vietnam revealed by DNA-based species
1039	delimitation analyses. Ecology and Evolution, 14: e11144.
1040	https://doi.org/10.1002/ece3.11144



1071

1041	Pons J, Barraclough TG, Gomez-Zurita J, Cardoso A, Duran DP, Hazell S, Kamoun S, Sumlin
1042	WD, Volger AP. 2006. Sequence based species delimitation for the DNA taxonomy of
1043	undescribed insects. Systematic Biology, 55(4): 595–609.
1044	https://doi.org/10.1080/10635150600852011
1045	Puillandre N, Brouillet S, Achaz G. 2021. ASAP: assemble species by automatic partitioning.
1046	Molecular Ecology Resources, 21(2): 609-620. https://doi.org/10.1111/1755-0998.13281
1047	Rambaut A. 2018. FigTree v1.4.4. Available at http://tree.bio.ed.ac.uk/software/figtree/ (accesed
1048	10 October 2023).
1049	Ramírez MJ. 2014. The morphology and phylogeny of dionychan spiders (Araneae:
1050	Araneomorphae). Bulletin of the American Museum of Natural History, 390: 1-374.
1051	http://dx.doi.org/10.1206/821.1
1052	Richardson BJ, Gunter NL. 2012. Revision of Australian jumping spider genus Servaea Simon
1053	1887 (Aranaea: Salticidae) including use of DNA sequence data and predicted
1054	distributions. Zootaxa, 3350(1): 1-33. https://doi.org/10.11646/zootaxa.3350.1.1
1055	Richman DB, Cutler B, Hill DE. 2012. Salticidae of North America, including Mexico.
1056	Peckhamia, 95(3): 1-88.
1057	Richman DB. 1981. A revision of the genus <i>Habrocestum</i> (Araneae, Salticidae) in North America.
1058	Bulletin of the American Museum of Natural History, 170: 197-206.
1059	Rosenzweig ML.1995.Species Diversity in Space and Time. UK: Cambridge University Press.
1060	https://doi.org/10.1017/CBO9780511623387
1061	Sbordoni V. 2010. Strength and Limitations of DNA Barcode under the Multidimensional Species
1062	Perspective. In: Nimis PL, Lebbe RV, ed. Tools for Identifying Biodiversity: Progress and
1063	Problems. Proceedings of the International Congress. Paris, Trieste: EUT Edizioni
1064	Università di Trieste.
1065	Schlick-Steiner BC, Steiner FM, Seifert B, Stauffer C, Christian E, Crozier RH. 2010. Integrative
1066	Taxonomy: A Multisource Approach to Exploring Biodiversity. Annual Review of
1067	Entomology, 55: 421-438. https://doi.org/10.1146/annurev-ento-112408-085432
1068	Stein A, Gerstner K, Kreft H. 2014. Environmental heterogeneity as a universal driver of species
1069	richness across taxa, biomes and spatial scales. Ecology Letters, 17(7): 866-80.

PeerJ reviewing PDF | (2024:07:104276:0:1:NEW 2 Aug 2024)

https://doi.org/10.1111/ele.12277

Takhtajan A. 1986. Floristic regions of the world. Berkeley, University of California Press.



1072 Trebicki Ł, Patoleta BM, Dabert M, Żabka M. 2021. Redescription of type species of the genus 1073 Cytaea Keyserling, 1882 (Araneae: Salticidae)—an integrative approach. The European 1074 Zoological Journal, 88(1), 933-947. https://doi.org/10.1080/24750263.2021.1961029 1075 USGS. 2021. North America Political Boundaries - Sciencebase-Catalog. Available at 1076 https://www.sciencebase.gov/catalog/item/4fb555ebe4b04cb937751db9 (accesed 16 1077 January 2024). 1078 Valdez-Mondragón A, Francke OF. 2015. Phylogeny of the spider genus *Ixchela Huber*, 2000 (Araneae: Pholcidae) based on morphological and molecular evidence (CO1 and 16S), with 1079 1080 a hypothesized diversification in the Pleistocene. Zoological Journal of the Linnean 1081 Society, 175: 20–58. https://doi.org/10.1111/zoj.12265 1082 Valdez-Mondragón A, Navarro-Rodríguez CI, Solís-Catalán KP, Cortez-Roldán MR, Juárez-Sánchez AR. 2019. Under an integrative taxonomic approach: The description of a new 1083 1084 species of the genus Loxosceles (Araneae, Sicariidae) from Mexico City. ZooKeys, 892: 93–133. https://doi.org/10.3897/zookeys.892.39558 1085 1086 Valdez-Mondragón A. 2013. Taxonomic revision of the spider genus *Ixchela Huber*, 2000 1087 (Araneae: Pholcidae), with description of ten new species from Mexico and Central America. Zootaxa, 3608 (5): 285–327. https://doi.org/10.11646/zootaxa.3608.5.1 1088 1089 Valdez-Mondragón A. 2020. COI mtDNA barcoding and morphology for species delimitation in 1090 the spider genus Ixchela Huber (Araneae: Pholcidae), with the description of two new 1091 species from Mexico. Zootaxa, 4747(1): 54-76. doi:10.11646/zootaxa.4747.1.2 1092 Valdivia-Ornela L, Castillo-Aja MR. 2001. Las regiones geomorfológicas del estado de Jalisco. 1093 Revista Geocalli, 2(3): 17-108. 1094 Valero-Padilla J, Rodríguez-Reynaga FP, Cruz-Angón A. 2017. Resumen ejecutivo. Contexto 1095 físico. In: Angón AC, Hermosillo, AO, Padilla JV, Melgarejo ED, ed. La biodiversidad en Jalisco. Estudio de Estado. Vol. I. México: CONABIO, 21-22. 1096 1097 Vink C, Dupérré N, McQuillan BN. 2011. The black-headed jumping spider, *Trite planiceps* Simon, 1899 (Araneae: Salticidae): redescription including cytochrome c oxidase subunit 1098 1099 1 and paralogous 28S sequences. New Zealand Journal of Zoology, 38(4): 317-331. 1100 http://dx.doi.org/10.1080/03014223.2011.613939 1101 WSC. 2024. World Spider Catalog. Version 24. Natural History Museum Bern. Available at 1102 http://wsc.nmbe.ch (accesed 27 April 2024). https://doi.org/10.24436/2

PeerJ

1103	Xu X, Liu F, Cheng R-C, Chen J, Xu X, Zhang Z, Ono H, Pham DS, Norma-Rashid Y, Arnedo
1104	MA, Kuntner M, Li D. 2015. Extant primitively segmented spiders have recently
1105	diversified from an ancient lineage. Proceedings of the Royal Society B: Biological
1106	Sciences, 282(1808): 20142486. https://doi.org/10.1098/rspb.2014.2486
1107	Yamasaki T, Yamaguchi M, Phung LTH, Huang PS, Tso IM. 2018. Redescription of Chrysilla
1108	lauta Thorell 1887 (Araneae: Salticidae) based on the comparison with the holotype, and
1109	DNA barcoding. Acta Arachnologica, 67(1): 23-29. http://dx.doi.org/10.2476/asjaa.67.23
1110	Zhang J, Kapli P, Pavlidis P, Stamatakis A. 2013. A general species delimitation method with
1111	applications to phylogenetic placements. Bioinformatics, 29(22): 2869-2876.
1112	https://doi.org/10.1093/bioinformatics/btt499
1113	Zhang J, Maddison WP. 2015. Genera of euophryine jumping spiders (Araneae: Salticidae), with
1114	a combined molecular-morphological phylogeny. Zootaxa, 3938(1): 1-147.
1115	https://doi.org/10.11646/zootaxa.3938.1.1



Table 1(on next page)

Specimens used in the molecular analyses under COI, DNA voucher numbers, localities, and GenBank/BOLD accession numbers.



1 Table 1. Specimens used in the molecular analyses under COI, DNA voucher numbers, localities, and

2 GenBank/BOLD accession numbers.

Specie	DNA voucher numbers	Locality	GenBank/BOLD
			accesion number
Naphrys pulex	Npulex_CAN1	Canada: Ontario	HM880192
	Npulex_CAN2	Canada: Wellintong	GU682819
	Npulex_CAN3	Canada: Wellintong	GU682817
	Npulex_CAN4	Canada: Wellintong	GU682816
	Npulex_CAN5	Canada: Wellintong	GU682814
	Npulex_CAN6	Canada: Wellintong	GU682836
	Npulex_CAN7	Canada: Wellintong	ARONT843-18
	Npulex_CAN8	Canada: Wellintong	ARONT876
	Npulex_CAN9	Canada: Ontario	ARONT917
	Npulex_CAN10	Canada: Wellintong	ARONT947
	Npulex_CAN11	Canada: Ontario	KP646979
	Npulex_CAN12	Canada: Ontario	KP656563
	Npulex_CAN13	Canada: Ontario	MG049224
	Npulex_CAN14	Canada: Ontario	ARONZ306
	Npulex_CAN15	Canada: Ontario	ARONZ331
	Npulex_CAN16	Canada: Ontario	ARONZ571
	Npulex_CAN17	Canada: Ontario	HQ924681
	Npulex_CAN18	Canada: Ontario	HQ924683
	Npulex_CAN19	Canada: Nova Scotia	GU683271
	Npulex_CAN20	Canada: Nova Scotia	GU683271
	Npulex_CAN21	Canada: Ontario	MF816087
	Npulex_CAN22	Canada: Nova Scotia	KP652066
	Npulex_CAN23	Canada: Quebec	KP646121
	Npulex_CAN24	Canada: Ontario	MF808927
	Npulex_CAN25	Canada: Ontario	MF816952
	Npulex_CAN26	Canada: Ontario	KP651428
	Npulex_CAN27	Canada: Ontario	KP648109
	Npulex_CAN28	Canada: Ontario	MF810509
	Npulex_CAN29	Canada: Ontario	ELPCG2846
	Npulex_CAN30	Canada: Ontario	ELPCG2847
	Npulex_CAN31	Canada: Ontario	ELPCG3050
	Npulex_CAN32	Canada: Ontario	ELPCG3523
	Npulex_CAN33	Canada: Ontario	ELPCG3524
	Npulex_CAN34	Canada: Ontario	ELPCG3525
	Npulex_CAN35	Canada: Ontario	ELPCG3599
	Npulex_CAN36	Canada: Ontario	ELPCG5003
	Npulex_CAN37	Canada: Ontario	ELPCG5472
	Npulex_CAN38	Canada: Ontario	ELPCG6449
	Npulex_CAN39	Canada: Ontario	ELPCG7399



Npulex_CAN40	Canada: Ontario	ELPCG7401
Npulex_CAN41	Canada: Ontario	ELPCG8416
Npulex_CAN42	Canada: Ontario	ELPCG8449
Npulex CAN43	Canada: Ontario	ELPCG8644
Npulex CAN44	Canada: Ontario	ELPCH2306
Npulex CAN45	Canada: Ontario	MG048013
Npulex CAN47	Canada: Nova Scotia	KP649884
Npulex CAN48	Canada: Nova Scotia	KP654153
Npulex_CAN49	Canada: Ontario	KP652349
Npulex_CAN50	Canada: Nova Scotia	MF809281
Npulex CAN51	Canada: Nova Scotia	MF813033
Npulex_CAN52	Canada: Ontario	OPPKG2671
Npulex_CAN53	Canada: Ontario	OPPOG1872
Npulex CAN54	Canada: Ontario	OPPZE1286
Npulex CAN55	Canada: Wellintong	KP647608
Npulex CAN56	Canada: Ontario	KM839902
Npulex CAN57	Canada: Ontario	JN308610
Npulex_CAN58	Canada: Ontario	JN308622
Npulex CAN59	Canada: Ontario	JN308631
Npulex CAN60	Canada: Ontario	JN308807
Npulex CAN61	Canada: Ontario	JN308822
Npulex_CAN62	Canada: Ontario	RARBB197
Npulex CAN63	Canada: Ontario	RARBB202
Npulex CAN64	Canada: Ontario	DQ127443
Npulex CAN65	Canada: Ontario	DQ127431
Npulex_CAN66	Canada: Ontario	RBGBB303
Npulex_CAN67	Canada: Ontario	ROUGE2474
Npulex_CAN68	Canada: Ontario	KT707577
Npulex CAN69	Canada: Ontario	KT707910
Npulex CAN70	Canada: Ontario	KT706489
Npulex CAN71	Canada: Ontario	KT619474
Npulex CAN72	Canada: Ontario	MG048049
Npulex CAN73	Canada: Ontario	MG046695
Npulex CAN74	Canada: Ontario	MG044990
Npulex CAN75	Canada: Ontario	HQ977049
Npulex CAN76	Canada: Ontario	KP650393
Npulex CAN77	Canada: Ontario	KP656197
Npulex CAN78	Canada: Ontario	KP646924
Npulex CAN79	Canada: Ontario	KP656484
Npulex_CAN80	Canada: Ontario	KP649929
Nnulex CAN81	Canada: Ontario	MG046512
Npulex_CAN81 Npulex CAN82	Canada: Ontario Canada: Ontario	MG046512 MG043132



	Npulex_CAN84	Canada: Ontario	MG509225
	Npulex_CAN85	Canada: Ontario	MG509777
	Npulex_CAN86	Canada: Ontario	KP656878
	Npulex_CAN87	Canada: Ontario	KP656232
	Npulex_USA2	United States: Texas	BBUSE1504
			(BIOUG01877-
			H01)
	Npulex_USA3	United States:	GMGSQ008
		Tennessee	(BIOUG03453-
			H09)
	Npulex_USA4	United States:	GMGST563
		Tennessee	(BIOUG04938-
			E01)
	Npulex_USA5	United States:	GMNCF099
		Washington	
	Npulex_USA6	United States: Unknown	OR235169
Naphrys xerophila	Nxerophila_USA1	United States: Texas	BBUSE1415
			(BIOUG01637-
			H07)
Naphrys sp.	Nsp_USA10	United States: High	OR174102
		Appalachian Mountains	
	Nsp_USA11	United States: High	OR173350
		Appalachian Mountains	
	Nsp_USA8	United States: High	OR174487
		Appalachian Mountains	
	Nsp_USA9	United States: High	OR174414
		Appalachian Mountains	
Naphrys echeri sp. nov.	Necheri_MEX11	Mexico: Michoacán	PP123908
	Necheri_MEX58	Mexico: Michoacán	PP123905
	Necheri_MEX71	Mexico: Michoacán	PP123902
	Necheri_MEX73	Mexico: Michoacán	PP123909
	Necheri_MEX74	Mexico: Michoacán	PP123903
	Necheri_MEX8	Mexico: Michoacán	PP123900
	Necheri_MEX9	Mexico: Michoacán	PP123901
Naphrys tecoxquin sp. nov.	Ntecoxquin_MEX109	Mexico: Jalisco	PP123899
	Ntecoxquin_MEX54	Mexico: Jalisco	PP123898
	Ntecoxquin_ MEX 56	Mexico: Jalisco	PP123906
Naphrys tuuca sp. nov.	Ntuuca_ MEX 52	Mexico: Nayarit	PP123904
	Ntuuca_ MEX 76	Mexico: Nayarit	PP123910
	Ntuuca_ MEX 98	Mexico: Nayarit	PP123907
Corticattus latus	Clatus_DomRep	Dominican Republic:	KC615698
		Pedernales	



Table 2(on next page)

Average genetic distances (p-distances) of COI among Naphrys species.



1 Table 2. Average genetic distances (*p*-distances) of COI among *Naphrys* species.

	1	2	3	4	5
1. Naphrys pulex USA	-				
2. Naphrys xerophila USA	11.8	-			
3. Naphrys sp. USA	15.1	16.4	-		
4. Naphrys tecoxquin sp. nov. MEX	14.0	12.9	18.1	-	
5. Naphrys echeri sp. nov. MEX	13.4	13.4	17.8	11.2	-
6. Naphrys tuuca sp. nov. MEX	13.0	13.6	17.2	11.0	11.1

2



Table 3(on next page)

Average genetic distance (p-distances) of COI within Naphrys species.

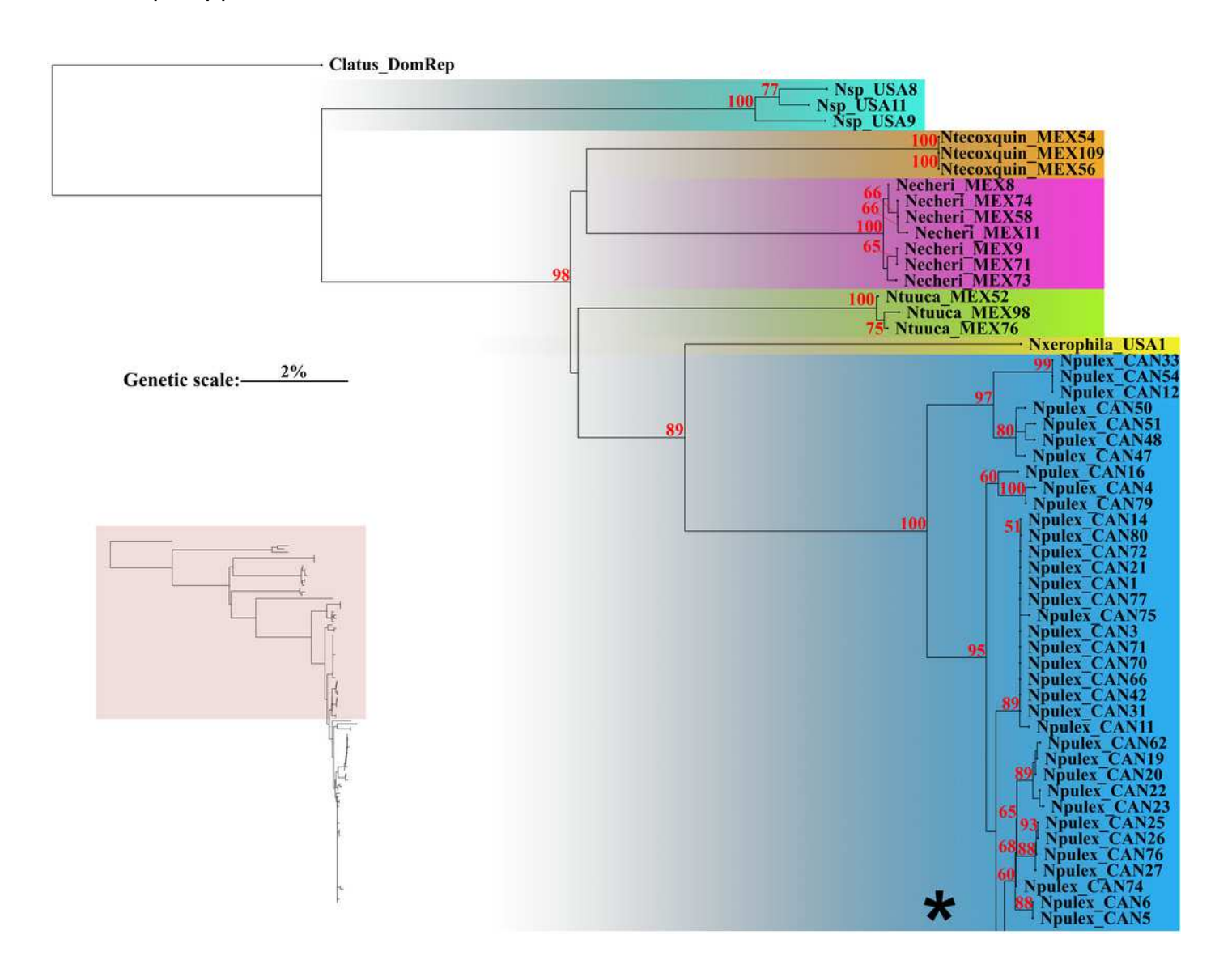


1 Table 3. Average genetic distance (*p*-distances) of COI within *Naphrys* species.

Specie	Distance	Standard	
		Error	
Naphrys pulex USA	1.61	0.26	
Naphrys xerophila USA	-	-	
Naphrys sp. USA	10.94	1.18	
Naphrys tecoxquin sp. nov. MEX	0	0	
Naphrys echeri sp. nov. MEX	0.32	0.15	
Naphrys tuuca sp. nov. MEX	0.34	0.19	

Neighbor-Joining (NJ) with corrected *p*-distances tree constructed with COI sequences from different species of *Naphrys*.

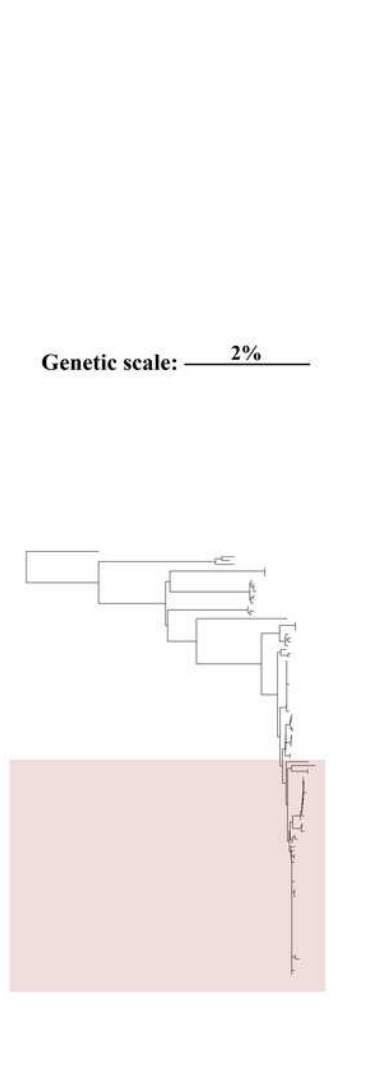
Colors indicate putative species. Red numbers above branches represent significant Bootstrap support values (> 50%).

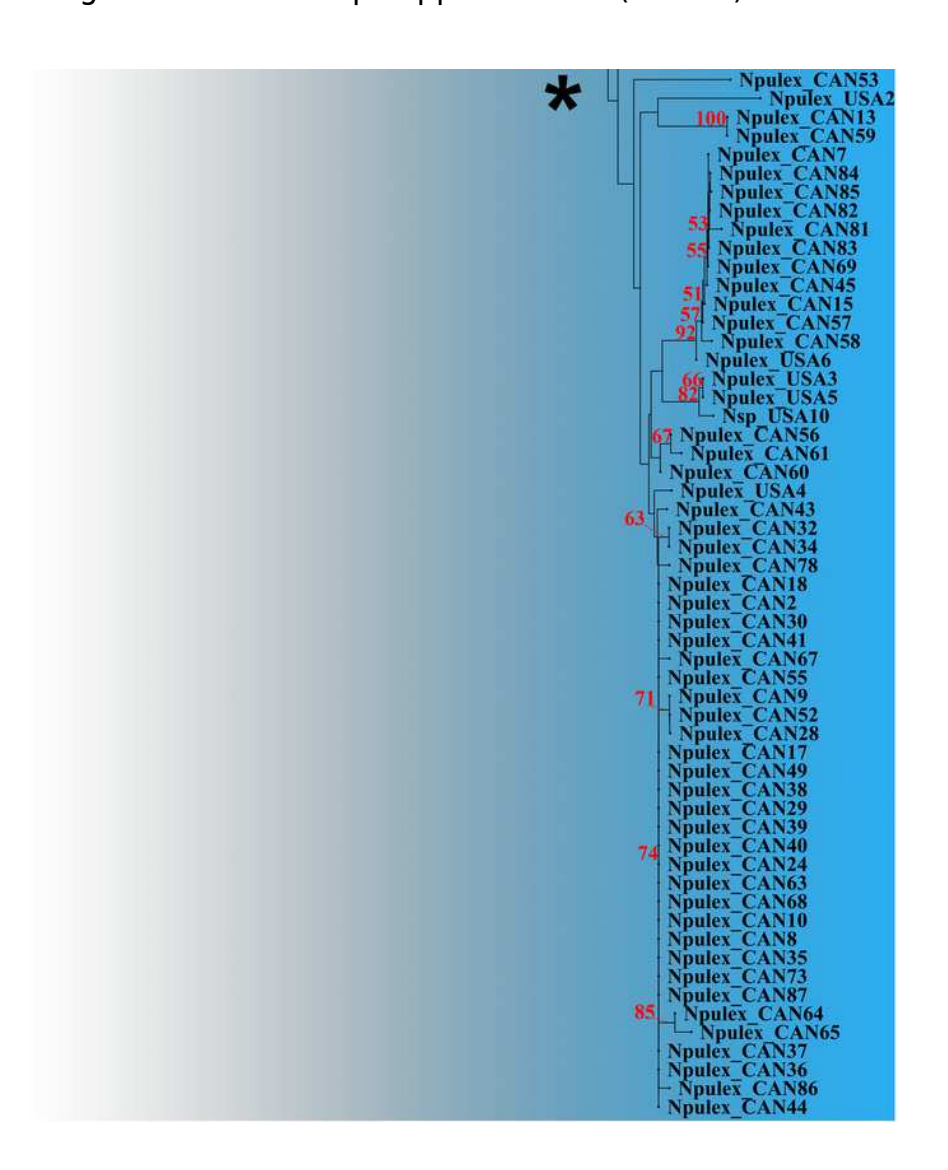




(Continued).

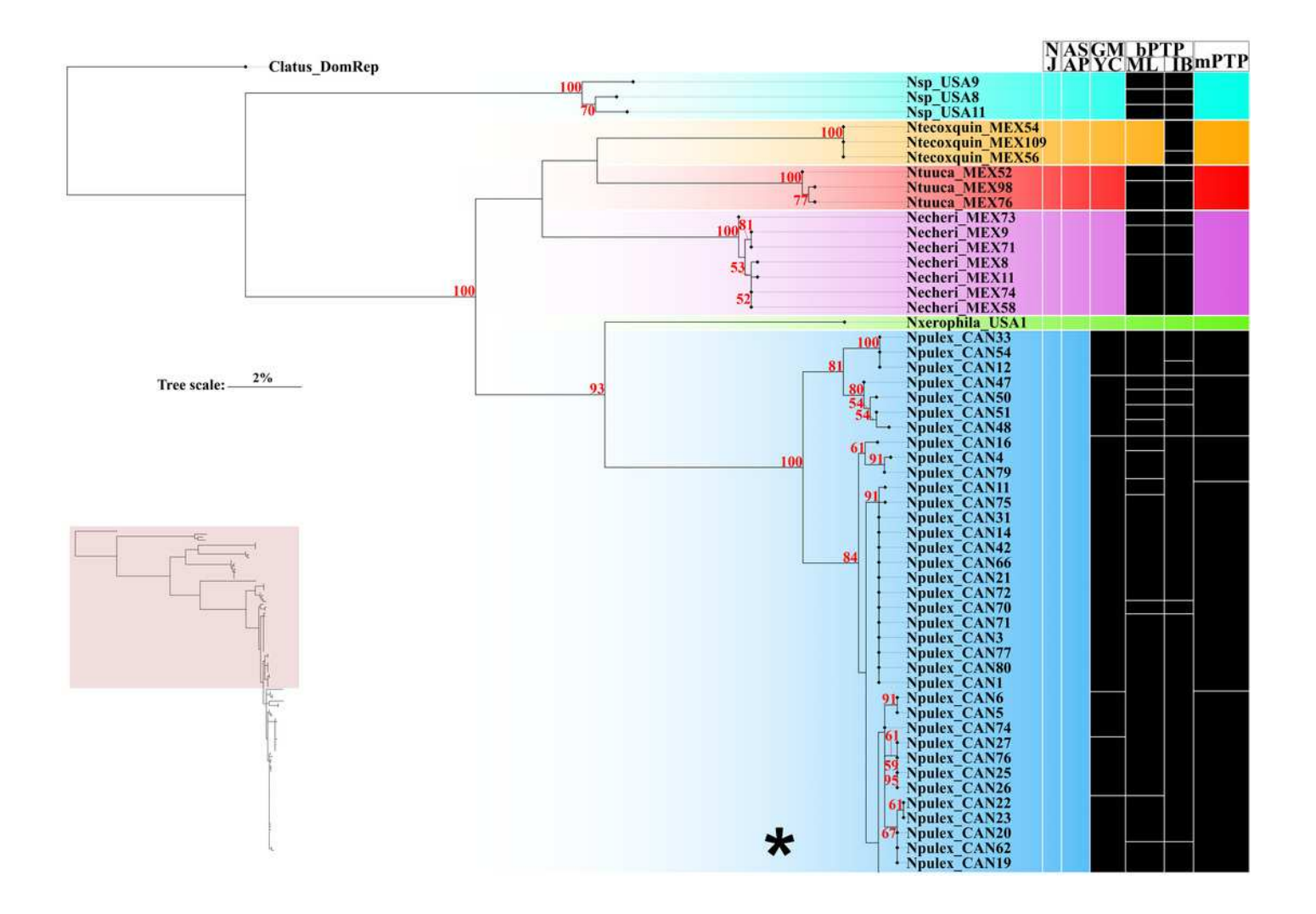
Image continuation of Neighbor-Joining (NJ) with corrected *p*-distances tree constructed with COI sequences from different species of *Naphrys*. Colors indicate putative species. Red numbers above branches represent significant Bootstrap support values (> 50%).





Maximum Likelihood (ML) tree of Naphrys constructed with COI.

Colors represent putative species. Columns represent the different species delimitation methods. Numbers above branches represent Bootstrap support values for ML (> 50% significant). Column abbreviations: Neighbor-Joining (NJ); General Mixed Yule Coalescent (GMYC); Bayesian Poisson Tree Processes (bPTP) with Maximum Likelihood (ML) and Bayesian Inference (IB) variants; Multi-rate Poisson Tree Processes (mPTP). Red numbers above branches represent Bootstrap support values for ML (> 50% significant).

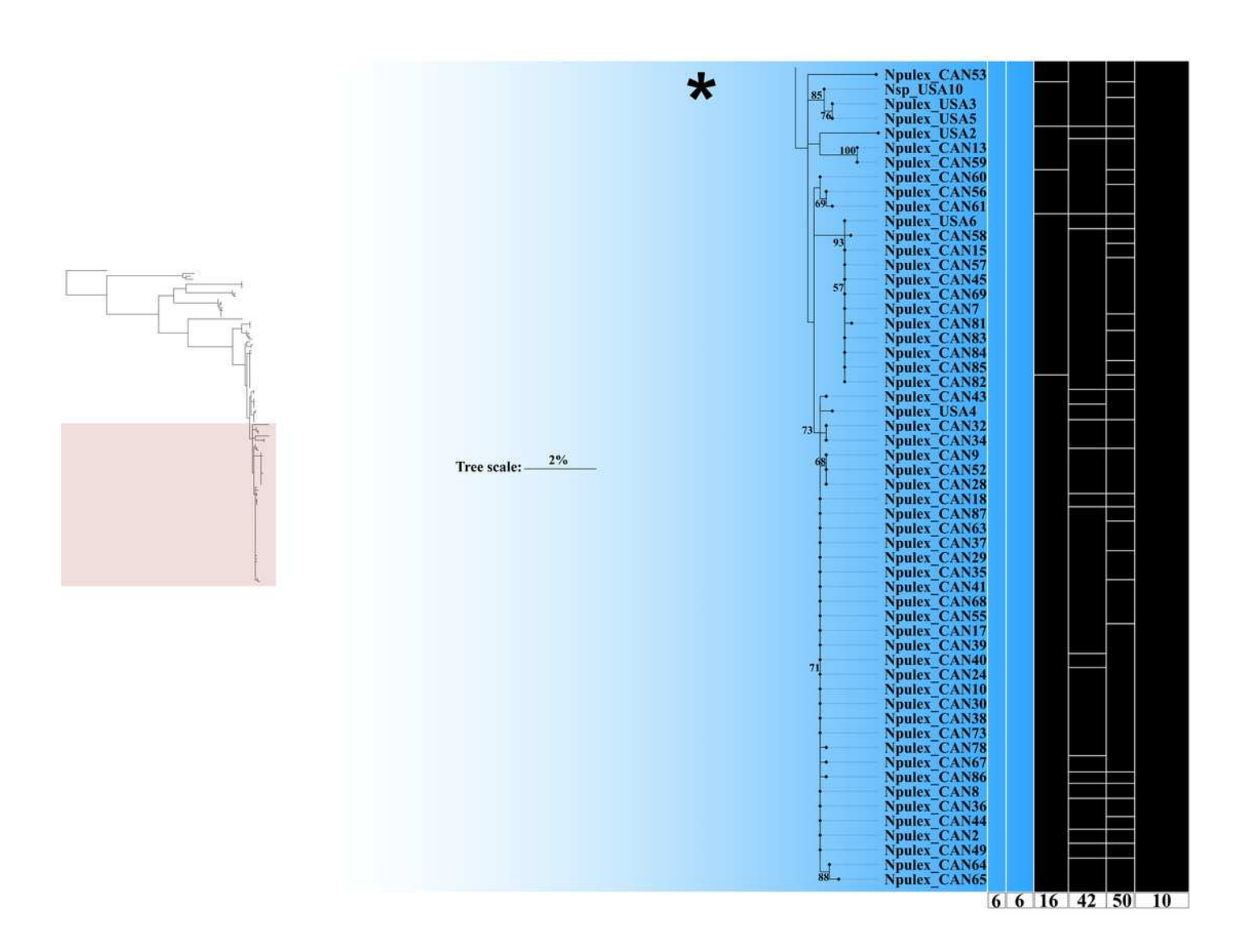




(Continued).

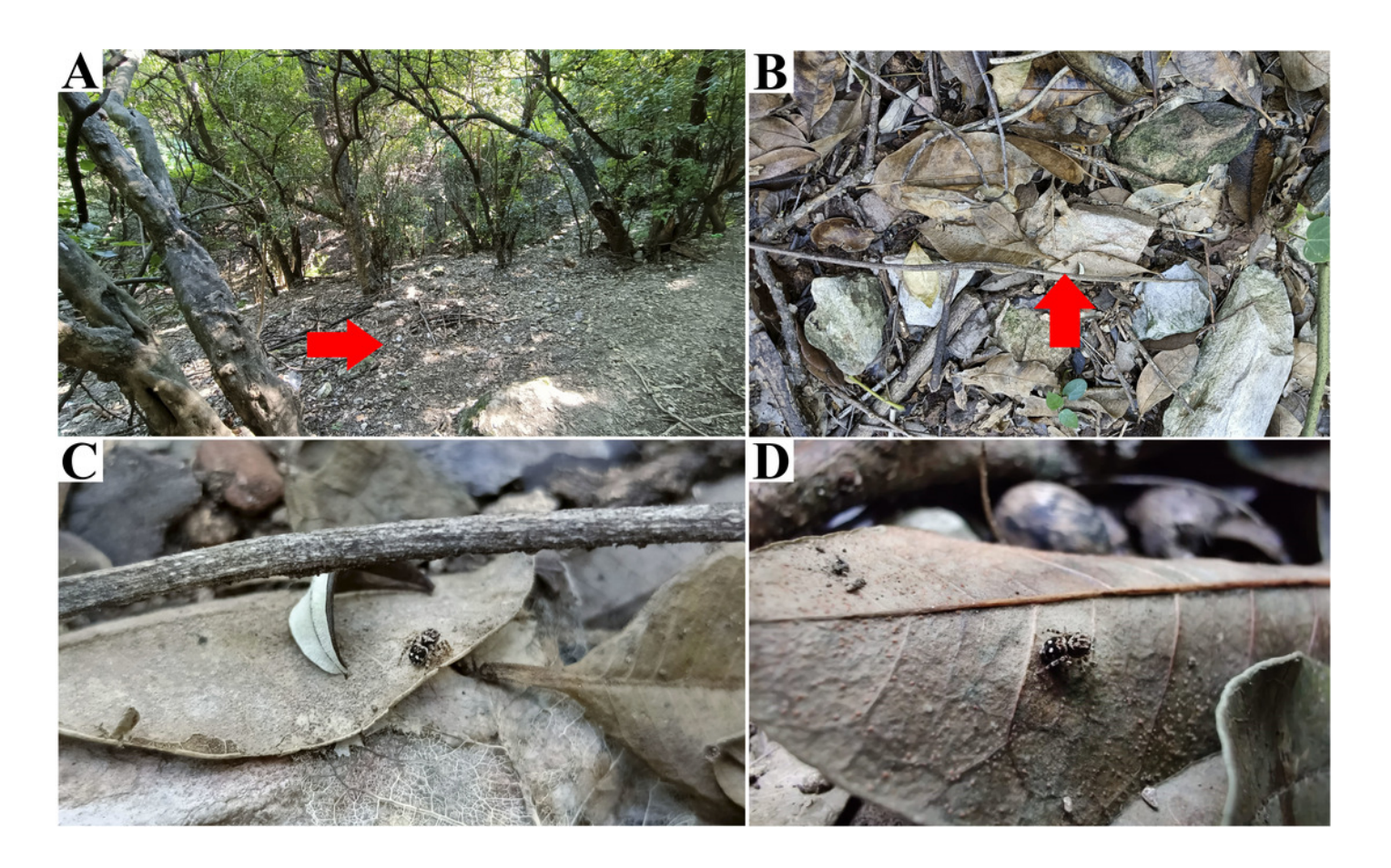
Image continuation of Maximum Likelihood (ML) tree of *Naphrys* constructed with COI. Colors represent putative species. Columns represent the different species delimitation methods. Numbers above branches represent Bootstrap support values for ML (> 50% significant). Column abbreviations: Neighbor-Joining (NJ); General Mixed Yule Coalescent (GMYC); Bayesian Poisson Tree Processes (bPTP) with Maximum Likelihood (ML) and Bayesian Inference (IB) variants; Multi-rate Poisson Tree Processes (mPTP). Red numbers above branches represent Bootstrap support values for ML (> 50% significant).





Naphrys acerba (Peckham & Peckham, 1909) from path to cable car, Cerro de la Silla, Guadalupe, Nuevo León, Mexico.

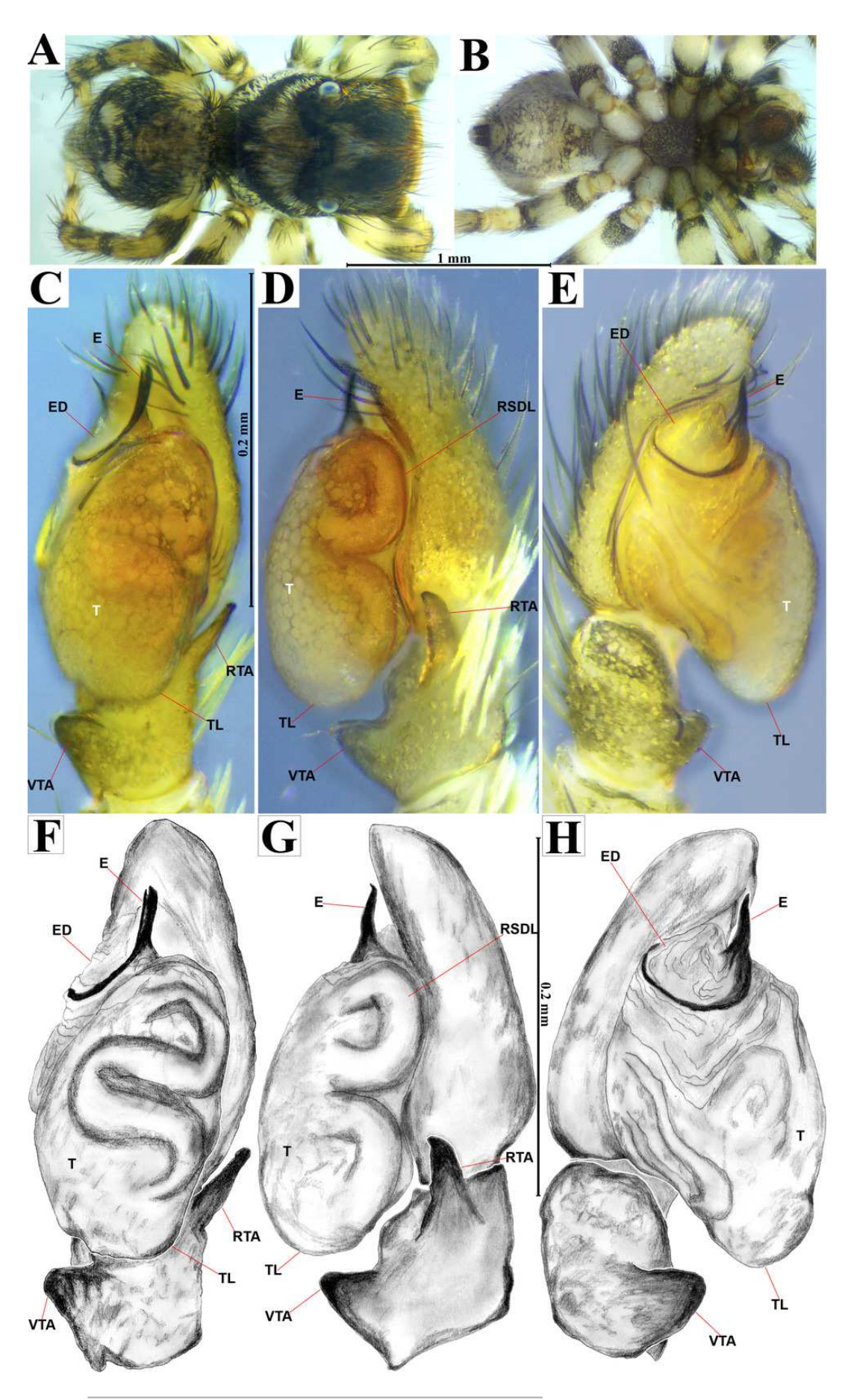
Red arrow indicates A) Habitat, B) Microhabitat. C) and D) Live female on leaf litter. Photos by Juan Maldonado-Carrizales (2023)





Naphrys acerba (Peckham & Peckham, 1909)

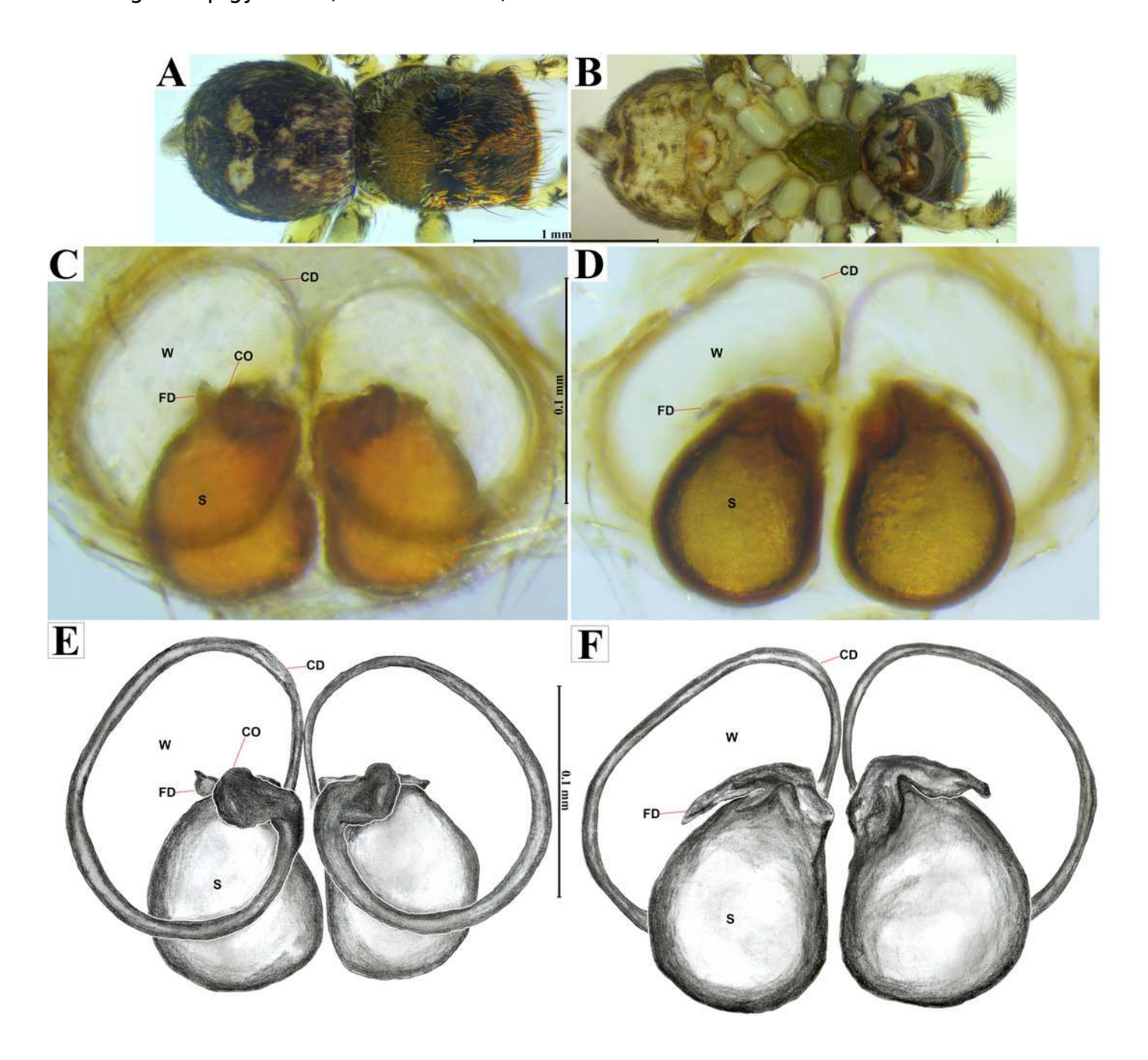
male habitus A) dorsal and B) ventral views. Left palp C) ventral, D) retrolateral and E) prolateral views. Drawings of left palp F) ventral, G) retrolateral and H) prolateral views.



PeerJ reviewing PDF | (2024:07:104276:0:1:NEW 2 Aug 2024)

Naphrys acerba (Peckham & Peckham, 1909)

female habitus A) dorsal and B) ventral views. Epigynum C) dorsal and D) ventral views. Drawings of epigynum E) ventral and F) dorsal views.



Type locality of *Naphrys echeri* sp. nov. from Cerro El Gigante, Jesús del Monte, Morelia, Michoacán, Mexico.

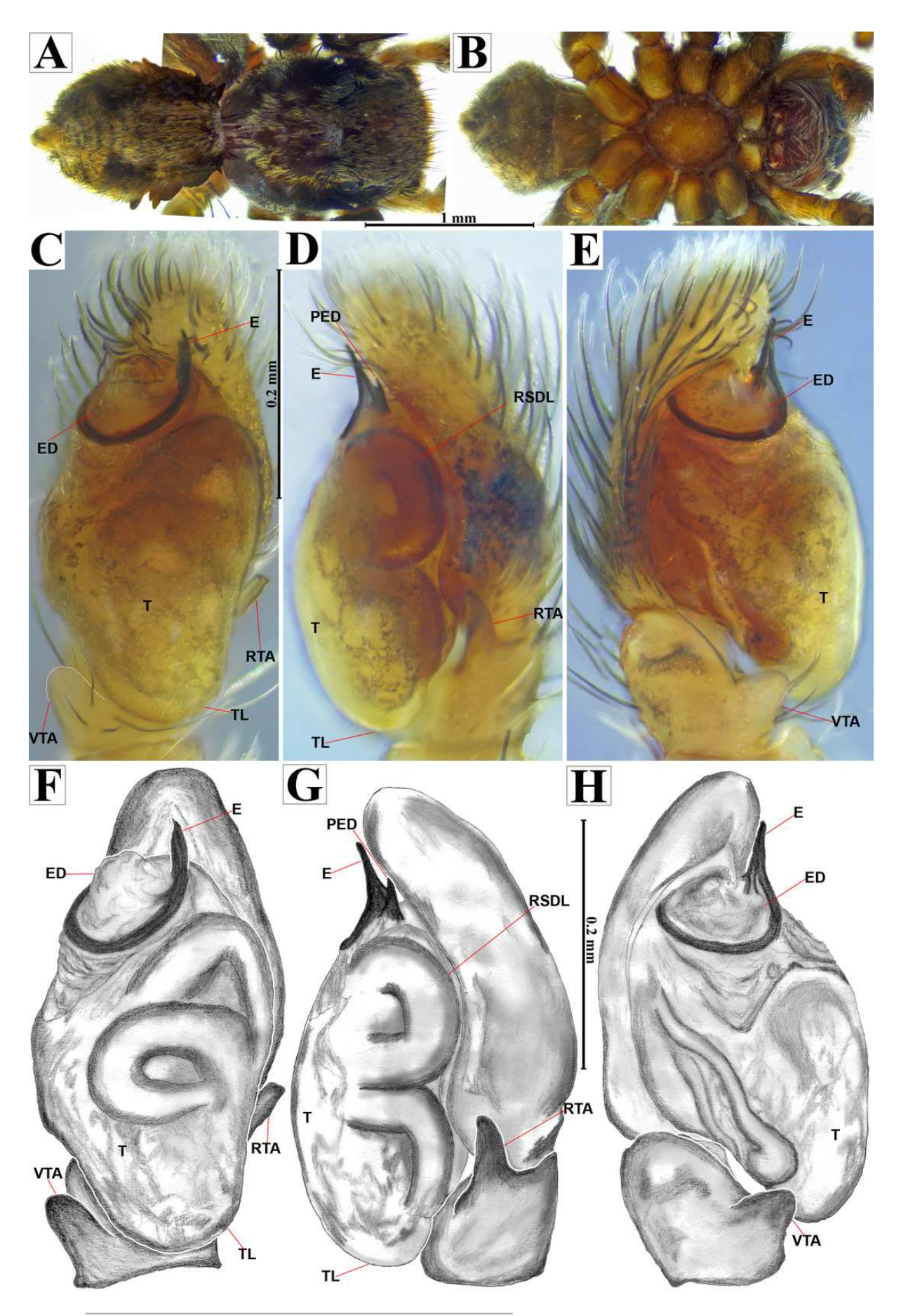
Red arrow indicates A) habitat and B) microhabitat. C) live female specimen in oak forest. Photos by Juan Maldonado-Carrizales (2023).





Naphrys echeri sp. nov. male holotype (CARCIB-AR-047)

habitus A) dorsal and B) ventral views. Left palp C) ventral, D) retrolateral and E) prolateral views. Drawings of left palp F) ventral, G) retrolateral and H) prolateral views.

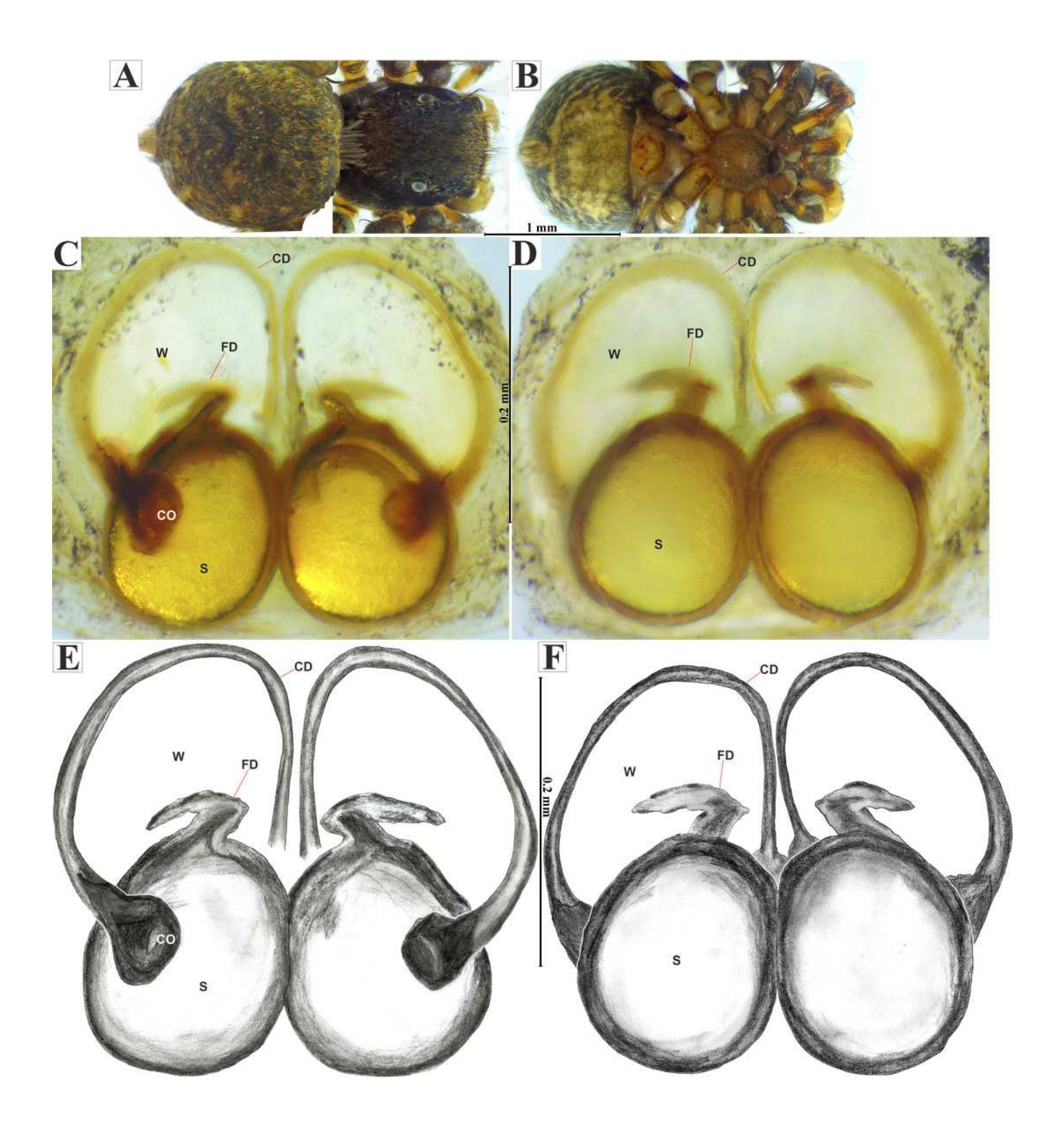


PeerJ reviewing PDF | (2024:07:104276:0:1:NEW 2 Aug 2024)



Naphrys echeri sp. nov. female allotype (CARCIB-Ar-008)

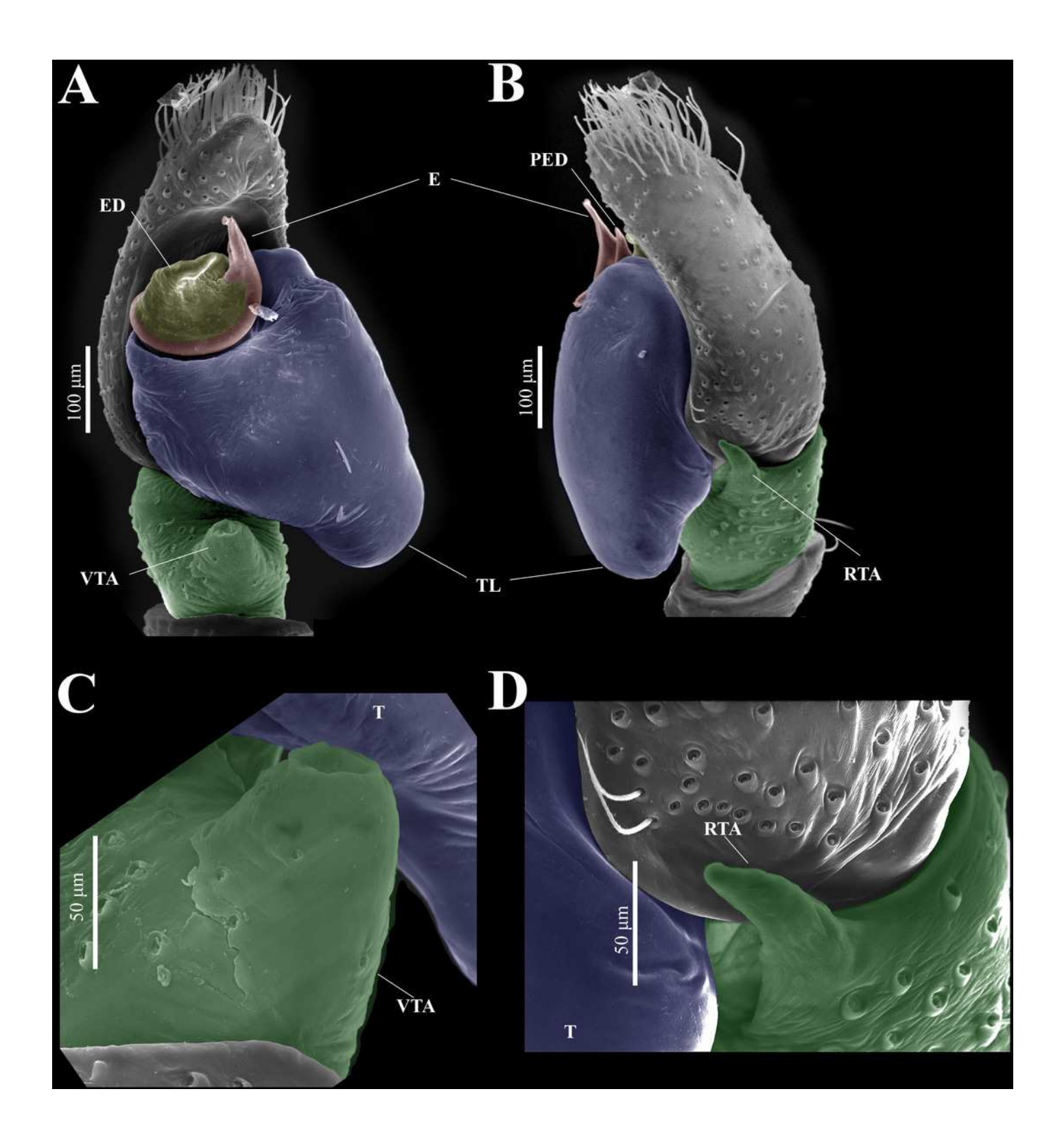
habitus A) dorsal and B) ventral views. epigynum C) dorsal and D) ventral views. Drawings of epigynum E) ventral and F) dorsal views.





Naphrys echeri sp. nov. male genitalia SEM micrographs.

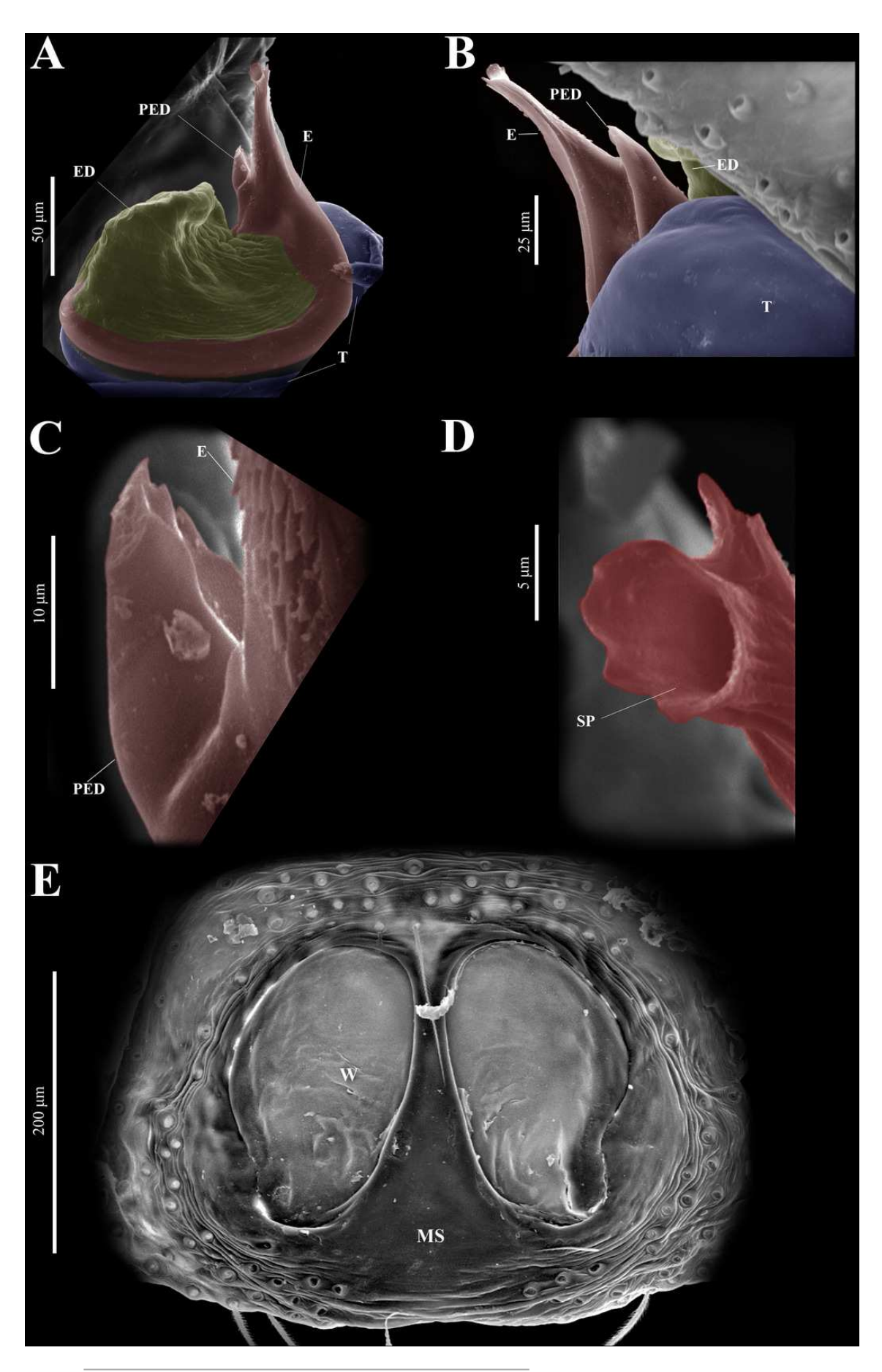
Palp A) prolateral and B) retrolateral views. C) ventral tibial apophysis (VTA). D) retrolateral tibial apophysis (RTA).





Naphrys echeri sp. nov. male genitalia SEM micrographs.

Embolus A) ventral and B) dorsal view. C) process on embolic disc (PED). D) sperm pore (SP) at embolus apex. E) female genitalia SEM micrograph epigynum ventral view.

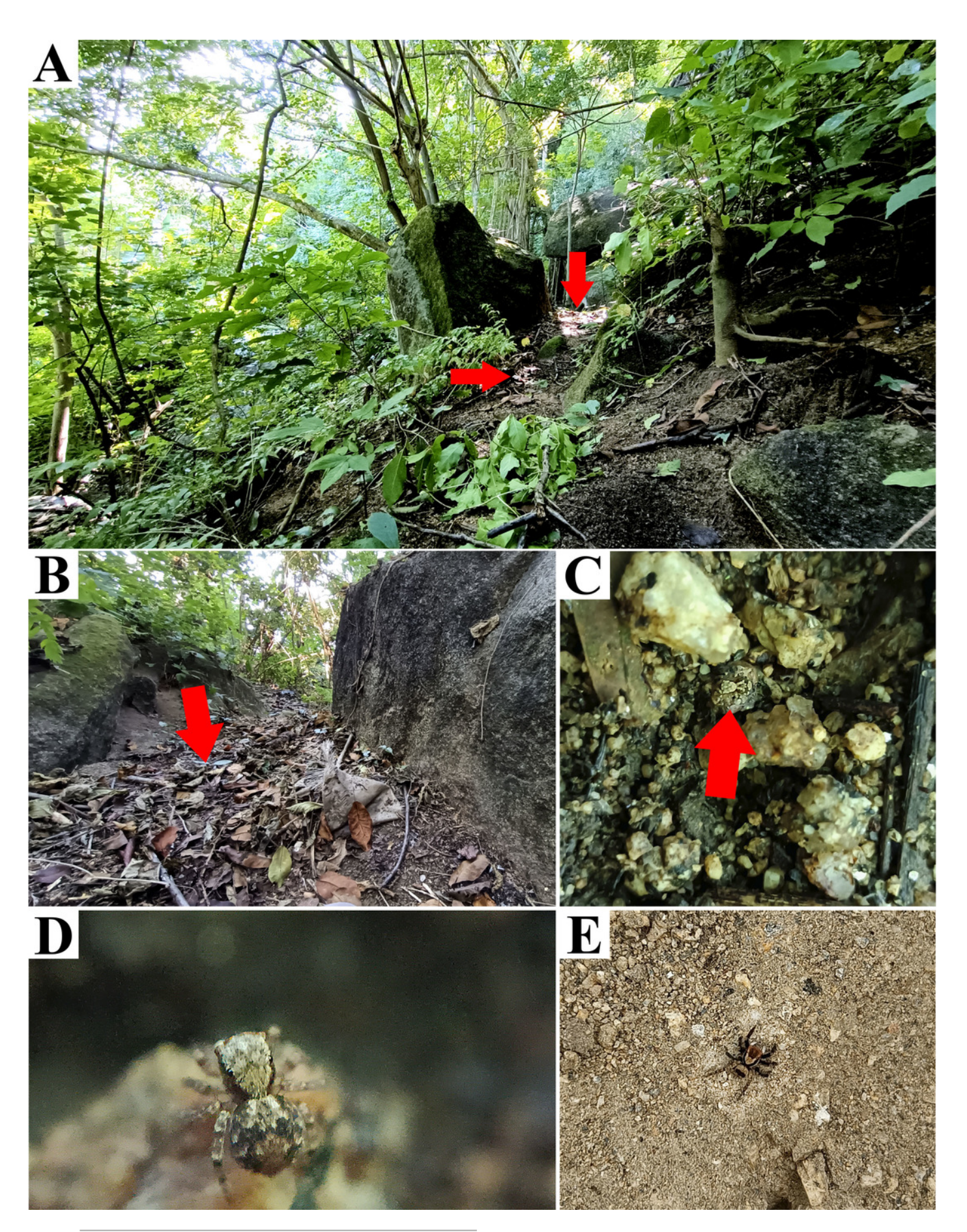


PeerJ reviewing PDF | (2024:07:104276:0:1:NEW 2 Aug 2024)



Type locality of *Naphrys tecoxquin* sp. nov. from Boca de Tomatlán, Cabo Corrientes, Jalisco, Mexico.

Red arrow indicates A) habitat and B) microhabitat. C) red arrow indicates live specimen on floor. D) female live specimen and E) male live specimen.

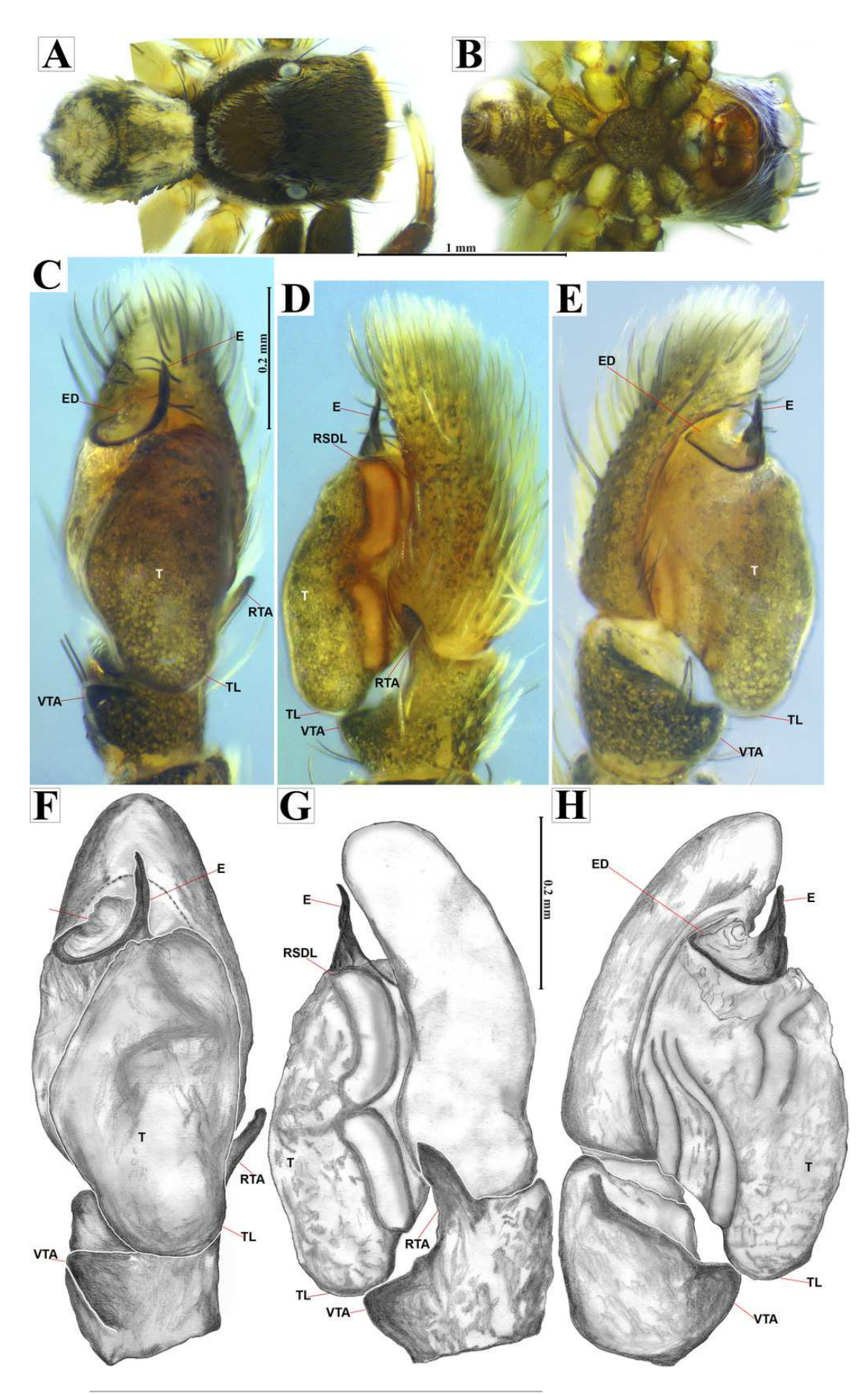


PeerJ reviewing PDF | (2024:07:104276:0:1:NEW 2 Aug 2024)



Naphrys tecoxquin sp. nov. male holotype (CARCIB-Ar-048)

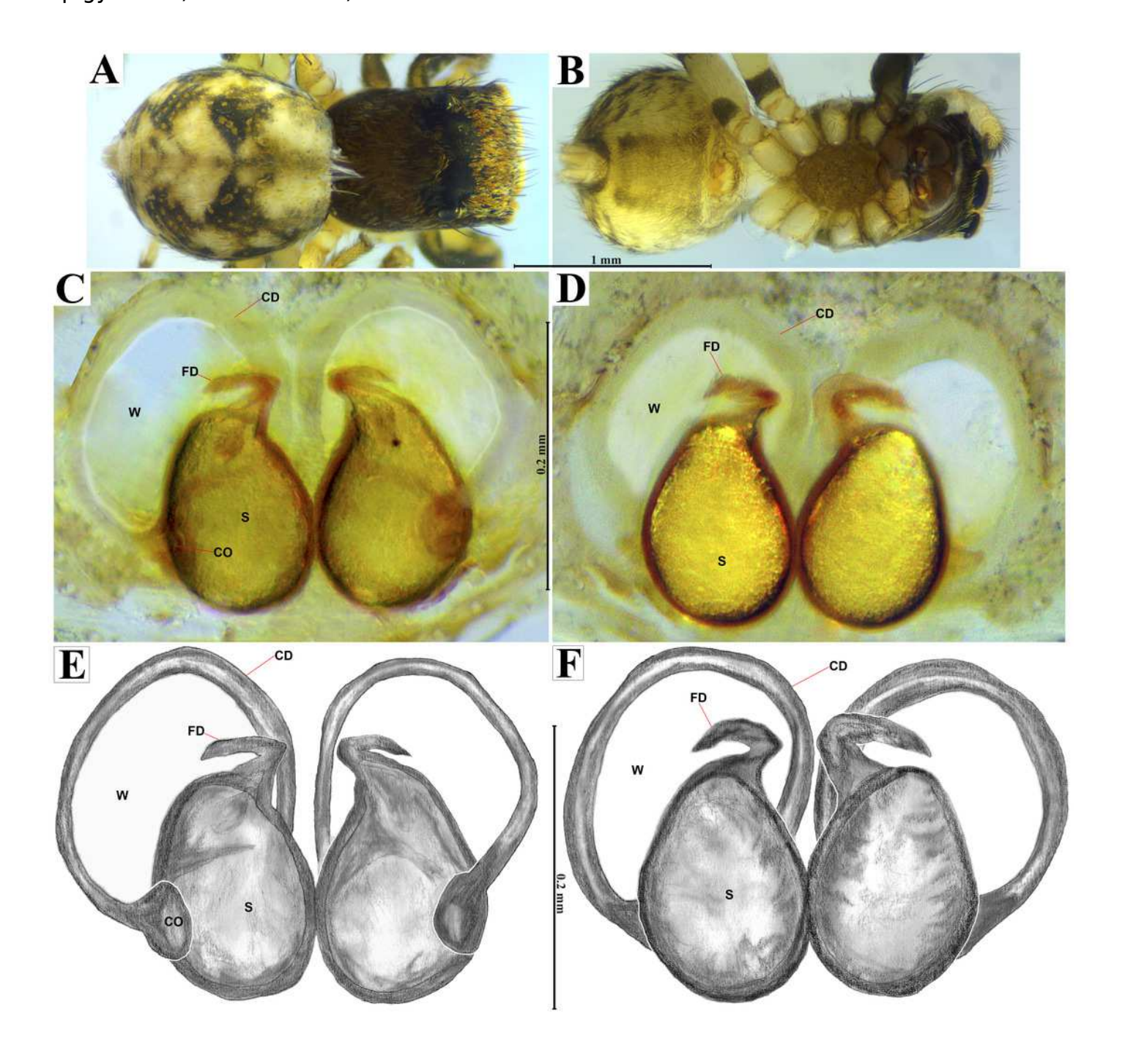
habitus A) dorsal and B) ventral views. Left palp C) ventral, D) retrolateral and E) prolateral views. Drawings of left palp F) ventral, G) retrolateral and H) prolateral views.



PeerJ reviewing PDF | (2024:07:104276:0:1:NEW 2 Aug 2024)

Naphrys tecoxquin sp. nov. female allotype (CARCIB-Ar-009)

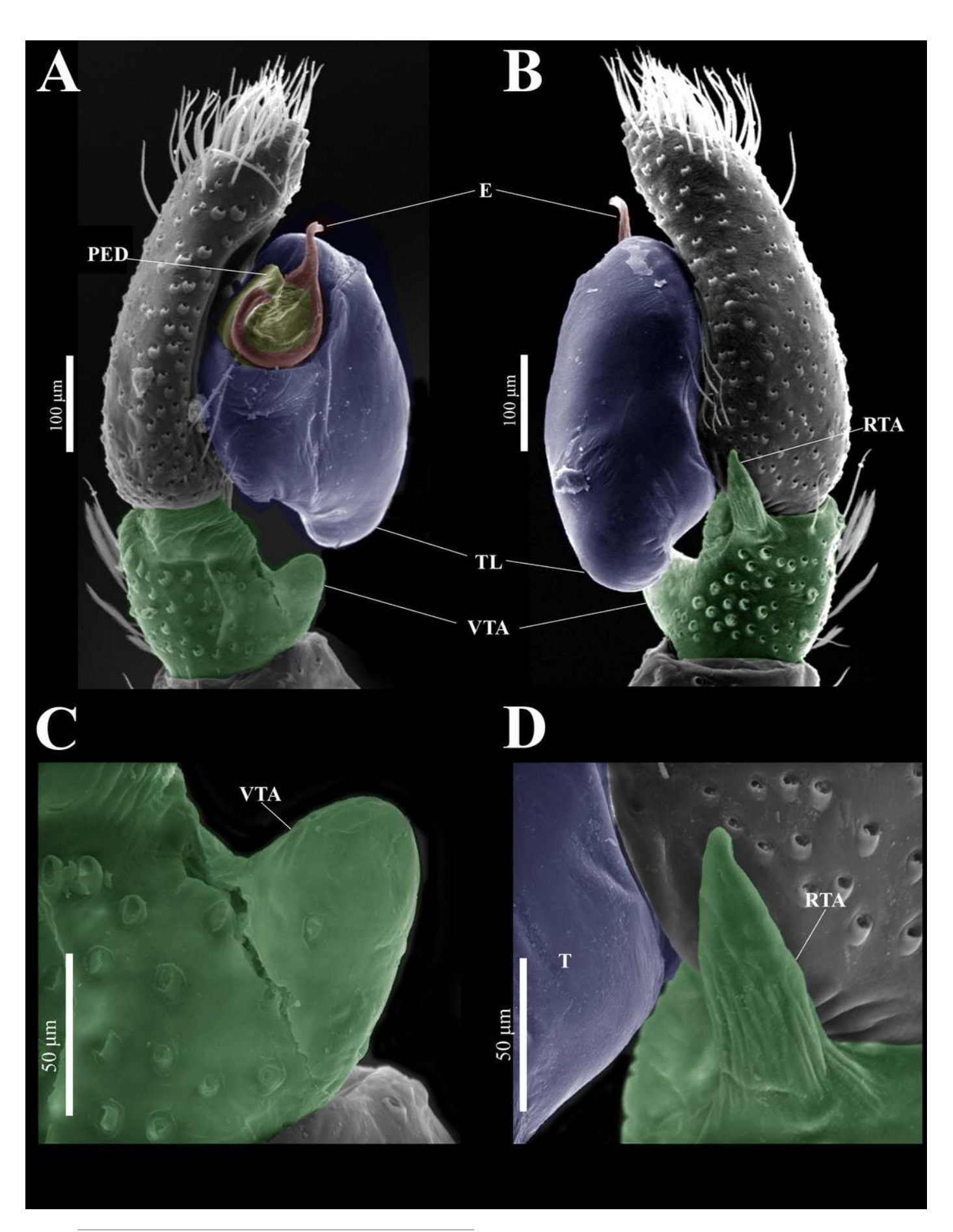
habitus A) dorsal and B) ventral views. epigynum C) dorsal and D) ventral views. Drawings of epigynum E) ventral and F) dorsal views.





Naphrys tecoxquin sp. nov. male genitalia SEM micrographs.

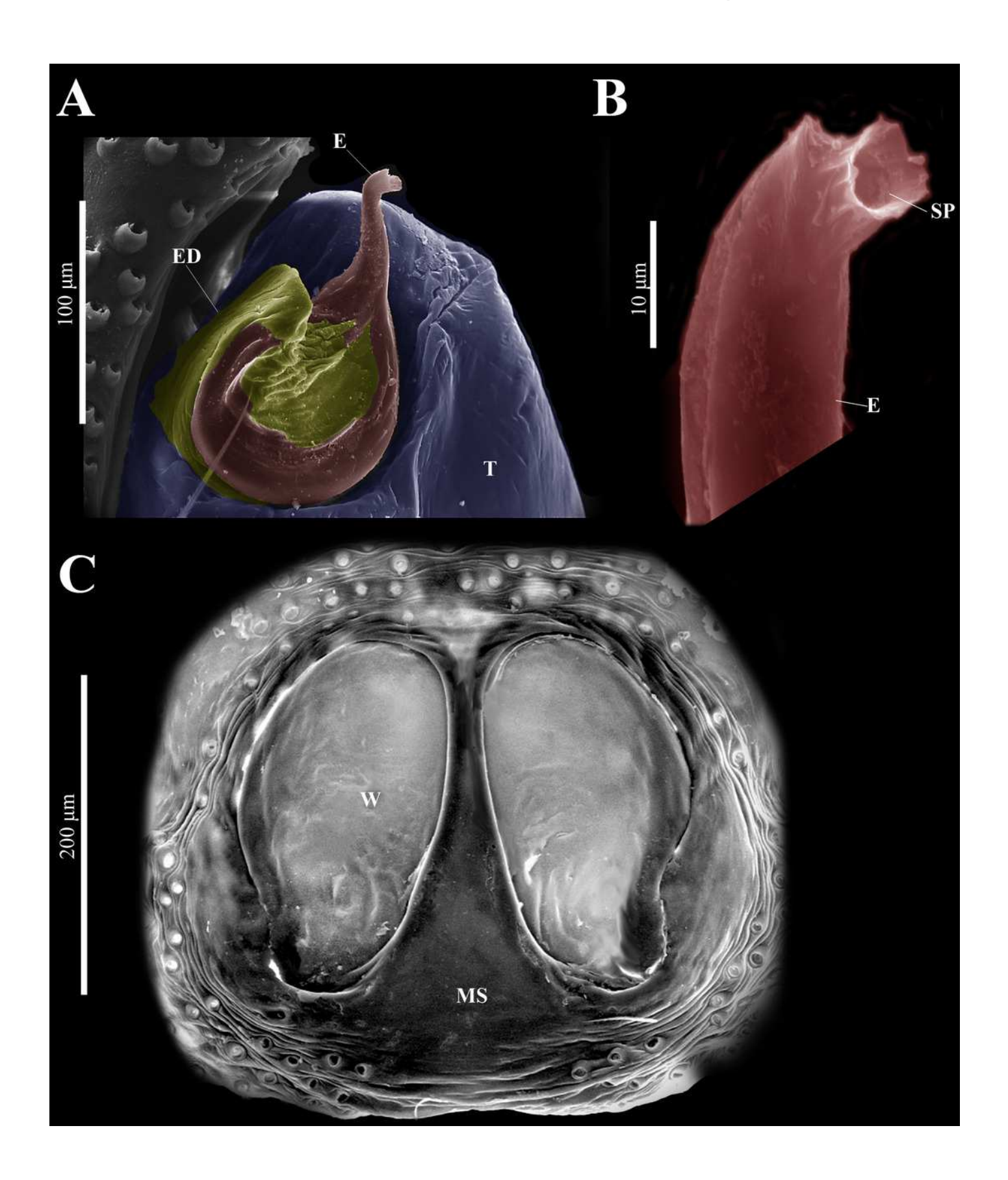
Palp A) prolateral and B) retrolateral views. C) ventral tibial apophysis (VTA). D) retrolateral tibial apophysis (RTA).





Naphrys tecoxquin sp. nov. male genitalia SEM micrographs.

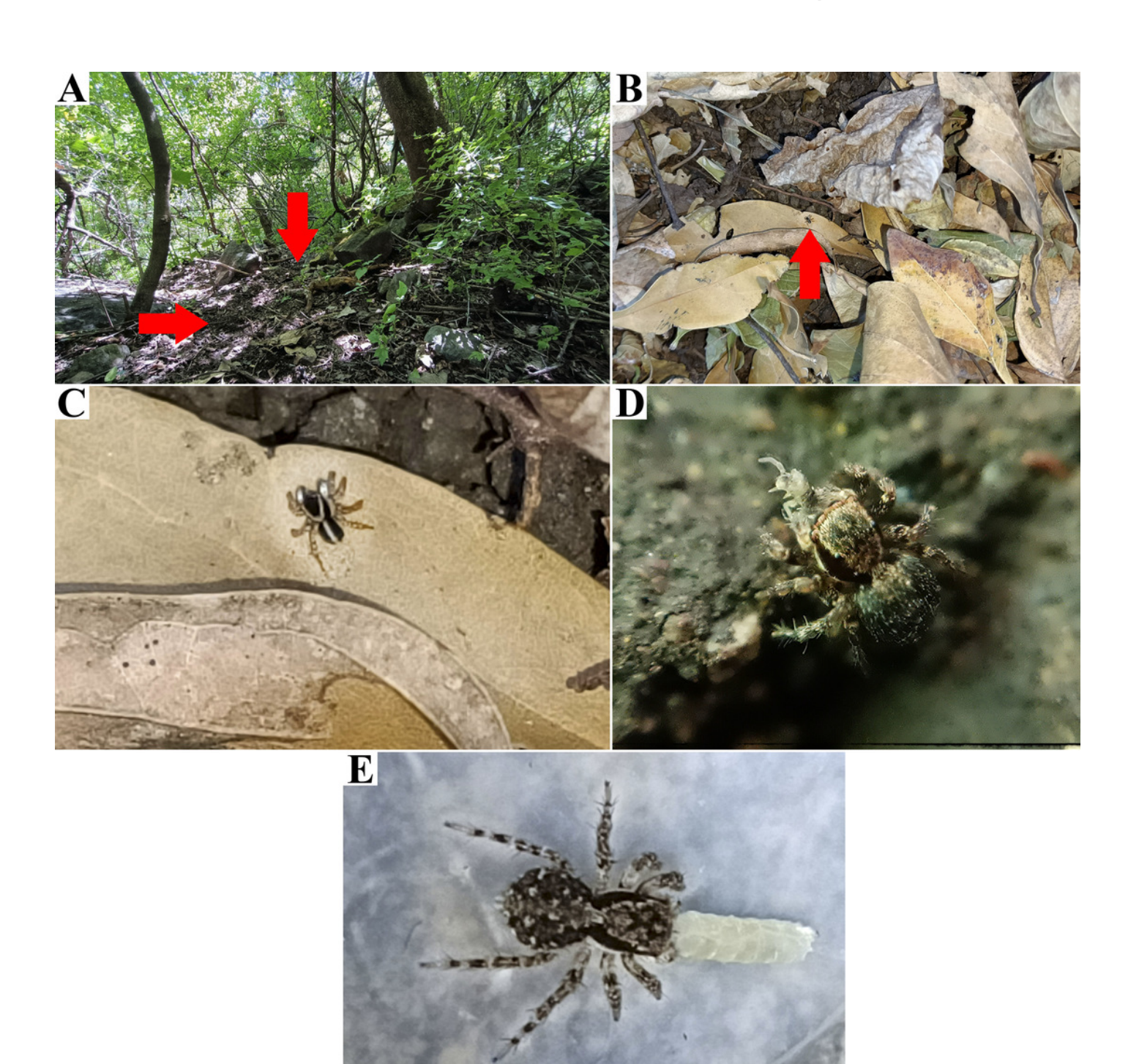
Embolus A) ventral view. B) sperm pore (SP) at embolus apex. C) female genitalia SEM micrograph epigynum ventral view.





Type locality of Naphrys tuuca sp. nov. from Cerro San Juan, Tepic, Nayarit, Mexico.

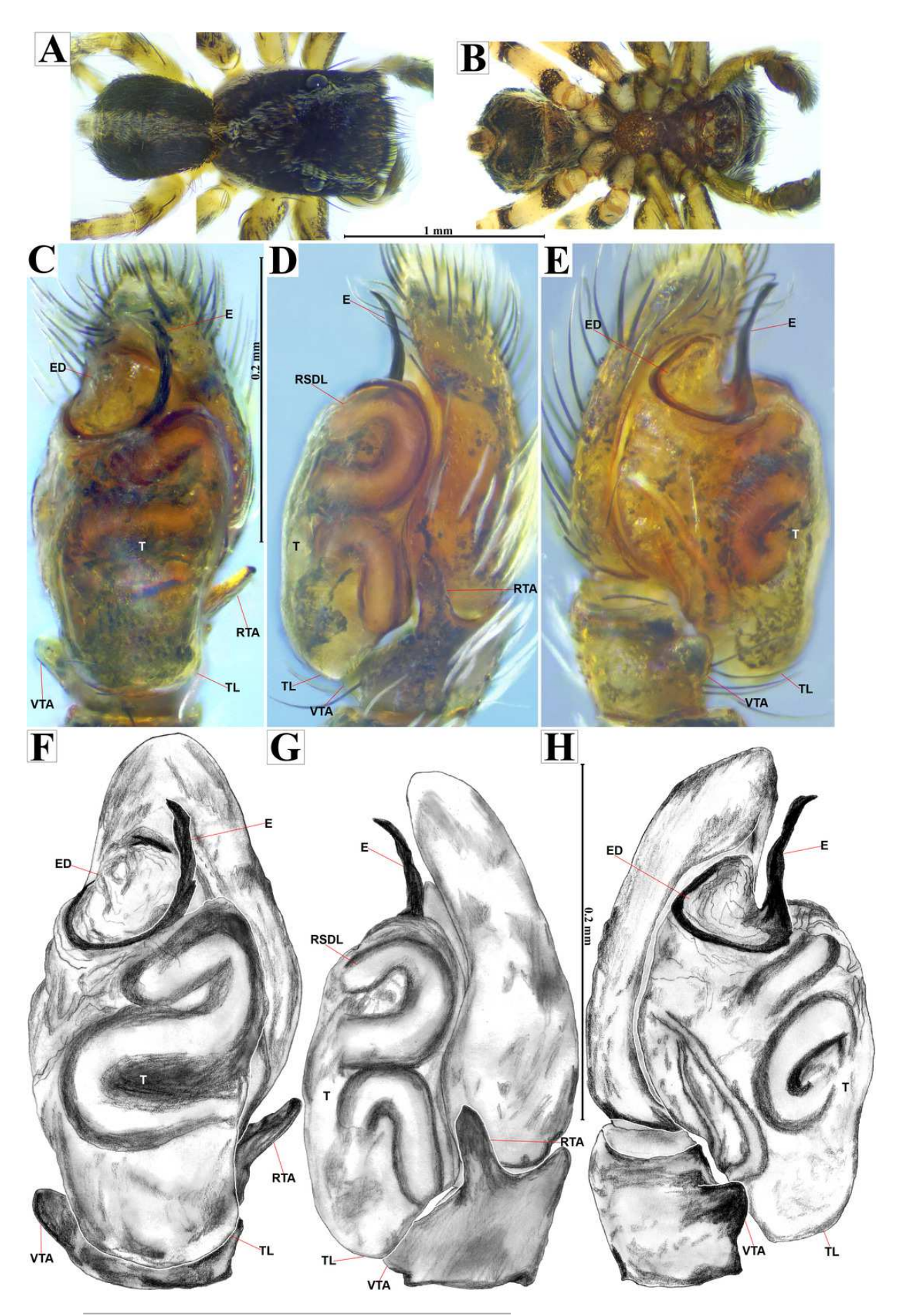
Red arrow indicates A) habitat and B) microhabitat. C) live male specimen. D) live female eating a Collembola in field. E) live female eating a larva of *Drosophila melanogaster* Meigen, 1830 in captivity. Photos by Juan Maldonado-Carrizales (2023).





Naphrys tuuca sp. nov. male holotype (CARCIB-Ar-049)

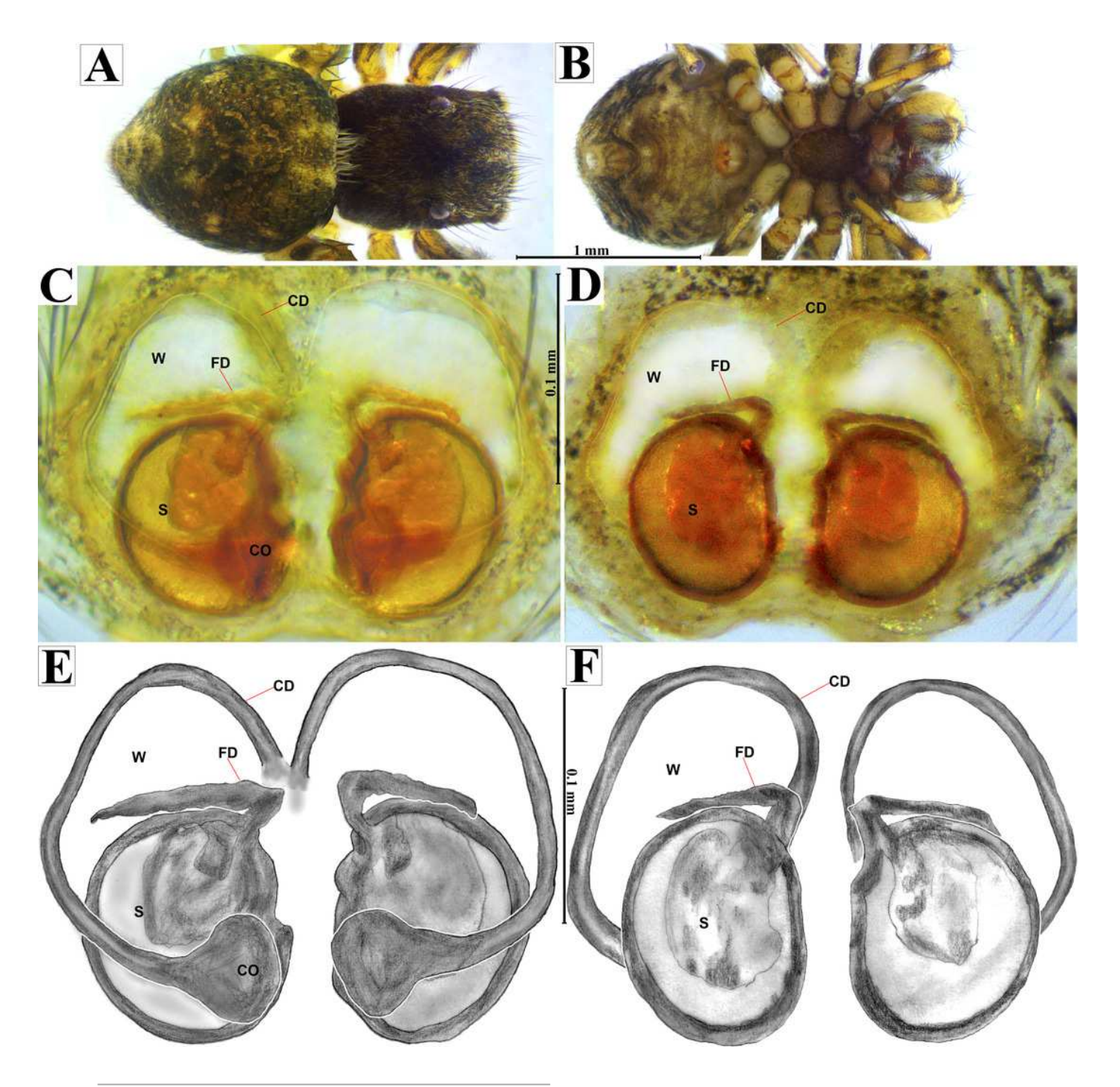
habitus A) dorsal and B) ventral views. Left palp C) ventral, D) retrolateral and E) prolateral views. Drawings of left palp F) ventral, G) retrolateral and H) prolateral views.



PeerJ reviewing PDF | (2024:07:104276:0:1:NEW 2 Aug 2024)

Naphrys tuuca sp. nov. female allotype (CARCIB-Ar-010)

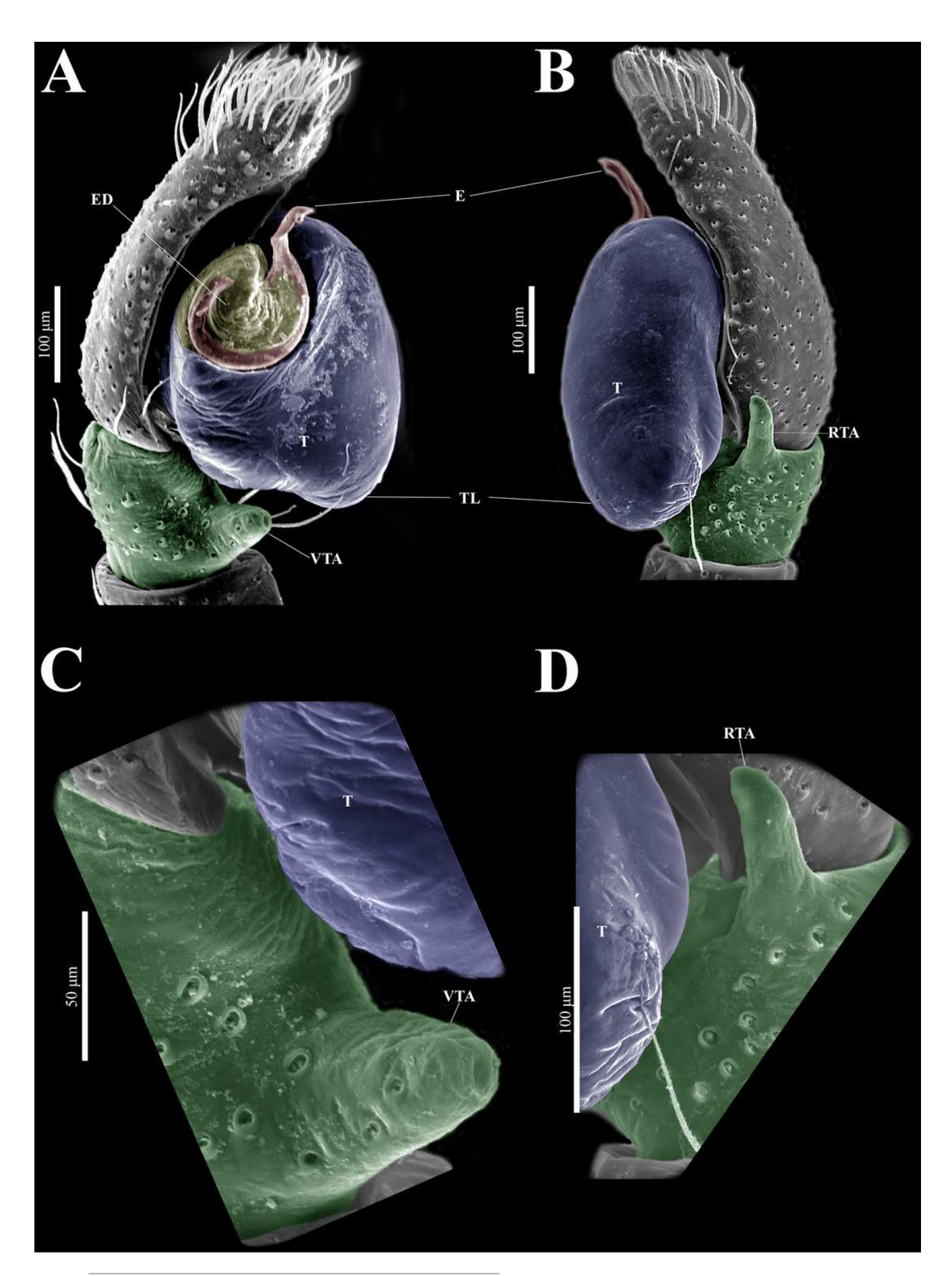
habitus A) dorsal and B) ventral views. epigynum C) dorsal and D) ventral views. Drawings of epigynum E) ventral and F) dorsal views.





Naphrys tuuca sp. nov. male genitalia SEM micrographs.

Palp A) prolateral and B) retrolateral views. C) ventral tibial apophysis (VTA). D) retrolateral tibial apophysis (RTA).

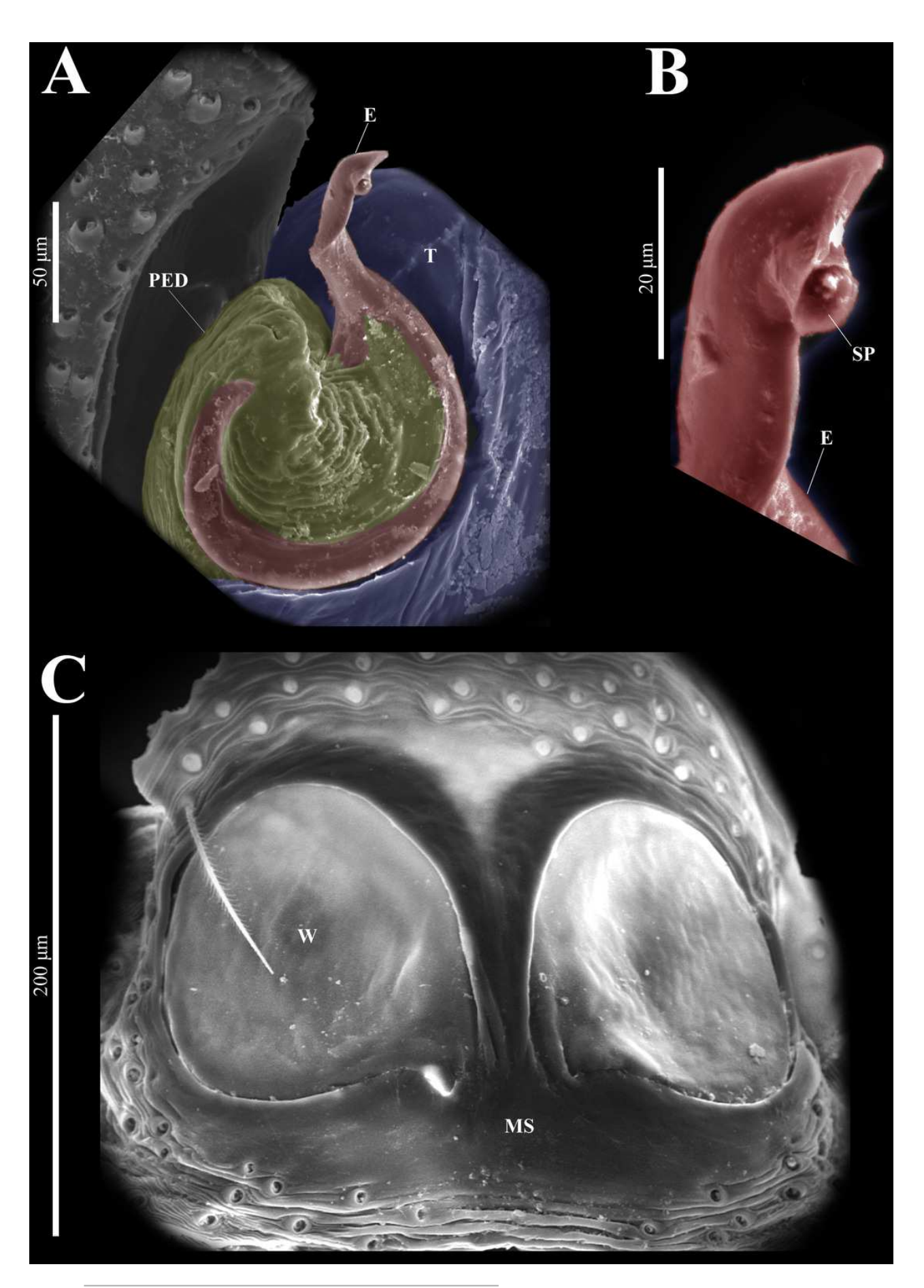


PeerJ reviewing PDF | (2024:07:104276:0:1:NEW 2 Aug 2024)



Naphrys tuuca sp. nov. male genitalia SEM micrographs.

Embolus A) ventral view. B) sperm pore (SP) at embolus apex. C) female genitalia SEM micrograph epigynum ventral view.



PeerJ reviewing PDF | (2024:07:104276:0:1:NEW 2 Aug 2024)

Known distribution records of the Mexican species of Naphrys.

Star: *N. acerba*. Diamond: *N. echeri* sp. nov.. Circle: *N. tecoxquin* sp. nov. Cross: *N. tuuca* sp. nov. Colors represent the biogeographical provinces following Escalante, Rodríguez-Tapia & Morrone (2021). Blue: Transmexican Volcanic Belt province. Green: Sierra Madre del Sur Province. Pink: Sierra Madre Oriental. Yellow: Pacific Lowlands.

